

THESIS FOR THE DEGREE OF DOCTOR IN PHILOSOPHY

NEW ANIONS FOR LITHIUM BATTERY ELECTROLYTES

Computational modelling and Raman spectroscopy

JOHAN SCHEERS



Department of Applied Physics  
CHALMERS UNIVERSITY OF TECHNOLOGY  
Göteborg, Sweden, 2011

# NEW ANIONS FOR LITHIUM BATTERY ELECTROLYTES

Computational modelling and Raman spectroscopy

JOHAN SCHEERS

© Johan Scheers, 2011

Doktorsavhandlingar vid Chalmers tekniska högskola

ISBN 978-91-7385-539-6

Ny serie nr: 3220

ISSN 0346-718X

Chalmers University of Technology

Department of Applied Physics

Condensed matter physics

SE-412 96 Göteborg

Sweden

Telephone: +46 (0)31-772 10 00

Fax: +46 (0)31-772 20 90

Cover:

The anions Bison, CSI, and CDI in the  
context of a dissociation-stability plot.

Printed by Chalmers Reproservice

Göteborg, Sweden, 2011

# NEW ANIONS FOR LITHIUM BATTERY ELECTROLYTES

Computational modelling and Raman spectroscopy

JOHAN SCHEERS

Department of Applied Physics  
Chalmers University of Technology

## ABSTRACT

Energy storage is crucial to realize a new global energy paradigm based on renewable energy sources. Batteries are well suited this need, with the advantages of being mobile and potentially environmentally benign. Li-ion batteries have revolutionized the market of portable electronics and are now being implemented as back up electricity for grid storage, and for transportation – powering hybrid and electric vehicles. However, for large scale applications, the safety of current Li-ion batteries is an obstacle. The safety problems of the Li-ion cell is inherent the reactivity of the choice of materials. Of particular concern, is the flammable organic electrolyte with the thermally unstable lithium hexafluorophosphate ( $\text{LiPF}_6$ ) salt. New salt alternatives must, in addition to high thermal stability, combine high electrochemical stability with facile  $\text{Li}^+$  transport.

In this thesis, alternatives to  $\text{LiPF}_6$  are explored by a combination of computational and spectroscopic techniques. The vertical transition energy,  $\Delta E_v$ , and ion pair dissociation energy,  $E_d$ , are computational approaches to the electrochemical stability of anions and the  $\text{Li}^+$ -anion interaction strength, respectively. From computationally predicted structures of anions and ion pair configurations, simulated vibration spectra can be compared with experimental Raman spectroscopic results to probe the molecular level environment of electrolytes. The lithium salts investigated can be categorized according to 1) their approximate geometric characteristics; linear, planar, or spherical, and 2) their substituents;  $-\text{F}$ ,  $-\text{CF}_3$ , or  $-\text{C}\equiv\text{N}$  groups.

The approach taken here is extremely idealized compared to the complex nature of real battery electrolytes; this is both a weakness and a strength. It will be further evaluated and modified based on future experimental results – implementation in lithium battery electrolytes.

Keywords: Batteries, electrolytes, ionic liquids, lithium salts, anions, *ab initio*, DFT, Raman spectroscopy



## LIST OF PUBLICATIONS

This thesis is based on the following papers:

- I. Anions for lithium battery electrolytes: A spectroscopic and theoretical study of the  $B(CN)_4^-$  anion of the ionic liquid  $C_2mim[B(CN)_4]$   
J. Scheers, P. Johansson, P. Jacobsson, *J. Electrochem. Soc.* 155 (2008) A628-A634.
- II. Benzimidazole and imidazole lithium salts for battery electrolytes  
J. Scheers, P. Johansson, P. Szczeciński, W. Wieczorek, M. Armand, P. Jacobsson, *J. Power Sources*, 195 (2010) 6081-6087.
- III. Novel lithium imides; the effects of  $-F$ ,  $-CF_3$ , and  $-C\equiv N$  substituents on lithium battery salt stability and dissociation  
J. Scheers, E. Jónsson, P. Jacobsson, P. Johansson, *Manuscript*.
- IV. Ion-ion and ion-solvent interactions in lithium imidazolid electrolytes studied by Raman spectroscopy and DFT models  
J. Scheers, L. Niedzicki, G.Z. Żukowska, P. Johansson, W. Wieczorek, P. Jacobsson, *Accepted for publication in Phys. Chem. Chem. Phys.* (2011).
- V. Ionic liquid and oligomer electrolytes based on the  $B(CN)_4^-$  anion; Ion association, physical and electrochemical properties  
J. Scheers, J. Pitawala, J.-K. Kim, F. Thebault, J.-H. Ahn, A. Matic, P. Johansson, P. Jacobsson, *Submitted to Phys. Chem. Chem. Phys.*

*Related paper not included in this thesis:*

Anion-Additive Interactions Studied by Ab Initio Calculations and Raman Spectroscopy

J. Scheers, M. Kalita, P. Johansson, G. Z. Żukowska, W. Wieczorek, P. Jacobsson, *J. Electrochem. Soc.* 156 (2009) A305-A308.

## CONTRIBUTION REPORT

- Paper I I (J.S.) performed the calculations and experiments, analyzed the data, and was the main author of the paper.
- Paper II J.S. performed the calculations, analyzed the data, and was the main author of the paper.
- Paper III J.S. planned the paper, performed the calculations, analyzed the data, and was the main author of the paper.
- Paper IV J.S. planned the paper, performed the calculations and experiments, analyzed the data, and was the main author of the paper.
- Paper V J.S. planned the paper, performed the Raman spectroscopic measurements and calculations, the corresponding data analyses, and was the main author of the paper.

## LIST OF ABBREVIATIONS

### **Materials**

Bison	Tetracyanoborate
BOB	Bis(oxalato)borate
DEC	Diethyl carbonate
DEE	Diethoxyethane
DFOB	Difluoro(oxalato)borate
DMC	Dimethyl carbonate
EMC	Ethyl methyl carbonate
FAB	Fluoroalkylborate
FAP	Fluoroalkylphosphate
FNSFI	(Fluorosulfonyl)(nonafluorobutanesulfonyl)imide
FSI	Bis(fluorosulfonyl)imide
LFP	Lithium fluoro phosphate
LTO	Lithium titanium oxide
PEO	Poly(ethylene oxide)
P(vDF-HFP)	Poly(vinylidene difluoride-hexafluoropropylene)
TADC	Dicyanotriazolate
TDI	Trifluoromethyl(dicyano)imidazolid
Tf	Trifluoromethanesulfonate
TFSI	Bis(trifluoromethanesulfonyl)imide
TOP	Tris(oxalato)phosphate

Additional anion acronyms can be found in papers I-III.

### **Computations**

B3LYP	Becke-(3-parameter), Lee, Yang, Parr (XC-functional)
C-PCM	Conductor-like polarizable continuum model
DFT	Density functional theory
GGA	Generalized gradient approximation
GTO	Gaussian-type orbital
HF	Hartree-Fock
HOMO	Highest occupied molecular orbital
LDA	Local density approximation
LUMO	Lowest unoccupied molecular orbital
MP2	Møller-Plesset 2 <sup>nd</sup> order (perturbation theory)
PCM	Polarized continuum method
PES	Potential energy surface
SAS	Solvent accessible surface
SCF	Self-consistent field
SES	Solvent excluded surface
STO	Slater-type orbital
VSXC	Voorhis-Scuseria exchange-correlation

## LIST OF ABBREVIATIONS (cont.)

### ***General***

CPE	Composite polymer electrolyte
DOD	Depth of discharge
EPW	Electrochemical potential window
EV	Electric vehicle
GPE	Gel polymer electrolyte
HEV	Hybrid electric vehicle
IL	Ionic liquid
LE	Liquid electrolyte
LPB	Lithium polymer battery
LSV	Linear sweep voltammetry
OCV	Open circuit voltage
PHEV	Plug-in hybrid electric vehicle
SEI	Solid electrolyte interphase
SEK	Swedish krona
SHE	Standard hydrogen electrode
SLI	Start-up lighting and ignition
SPE	Solid polymer electrolyte
SPI	Solid permeable interface
USD	United states dollars

# Table of Contents

<b>1</b>	<b>INTRODUCTION</b>	<b>1</b>
<b>2</b>	<b>BACKGROUND</b>	<b>3</b>
	2.1 Battery concepts	3
	2.2 Electrodes and interfaces	5
	2.3 Electrolytes	10
	2.4 Lithium salts	15
	2.5 Scope of thesis	21
<b>3</b>	<b>METHODS</b>	<b>23</b>
	3.1 Computations	23
	3.2 Raman Spectroscopy	32
<b>4</b>	<b>SUMMARY OF RESULTS</b>	<b>35</b>
	4.1 Ion pair dissociation and anion stability	35
	4.2 Ion interactions in LiTDI and XBison electrolytes	37
<b>5</b>	<b>CONCLUSIONS AND OUTLOOK</b>	<b>41</b>
<b>R</b>	<b>REFERENCES</b>	<b>43</b>
<b>A1</b>	<b>ACKNOWLEDGEMENT</b>	<b>51</b>
<b>A2</b>	<b>APPENDIX</b>	<b>53</b>
	Li-ion batteries – application status	53

## LIST OF SUBSECTIONS

### 2.1 Battery concepts

*Performance characteristics*

*Rechargeable battery systems*

*Li-ion battery operation mechanism*

### 2.2 Electrodes and interfaces

*Anodes and the anode/electrolyte interface*

*Cathodes and the cathode/electrolyte interface*

*Anode vs. cathode electrolyte interfaces*

### 2.3 Electrolytes

*Liquid and gel electrolytes*

*Solid polymer electrolytes*

*Ionic liquid based electrolytes*

### 2.4 Lithium salts

*Classic lithium salts*

*Thermal stability of  $\text{LiPF}_6$ -electrolytes*

*Alternative lithium salts*

*LITHIUM BORATES AND PHOSPHATES*

*LITHIUM METHIDE AND IMIDES*

*HETEROCYCLIC CYANO BASED LITHIUM SALTS*

### 3.1 Computations

*Wavefunction methods*

*Density functional methods*

*Continuum-solvent models*

*Basis Sets*

*Computed Molecular Properties*

*ANION OXIDATION STABILITY*

*ION PAIR DISSOCIATION ENERGY*

# 1 INTRODUCTION

This thesis comprises work on materials for rechargeable lithium batteries, today well-developed power sources for consumer electronics, and at the brink of expanding into new and exciting large scale application areas. In the following, an outlook is presented of the challenges and opportunities that exist for batteries in general. This outlook expands far out from the narrow theme of this thesis, but provides the necessary horizon of expectations that drives research on battery materials and battery engineering.

In view of the current environmental awareness, a future for batteries is as an integral part of a sustainable global energy solution, where the dependence on fossil fuels is relieved in favour of renewable energy sources. This change is motivated by increased worldwide energy utilization, finite fossil fuel reserves, and global environmental effects, such as air pollution and climate changes, connected with the current global energy situation. Relying on wind and solar plants for future electricity generation there is an increased demand for energy storage systems that can provide back-up electricity – load levelling of the electric grid – when the wind is not blowing or the sun is blocked. Compared to hydro-electric storage and other geographically constrained storage systems, the size and mobility of alternative battery installations are to their advantage.

For the transportation section, a battery powered electrical engine can support or possibly replace a combustion engine, with the advantage of minimizing exhaust gases. This trend is already well underway, with an increasing number of hybrid electrical vehicles (HEVs) on the street. HEVs offer improved fuel economics and are now also supplemented by plug-in hybrid electrical vehicles PHEVs. The latter can for a short distance ( $\sim 65 \text{ km}$ )<sup>1</sup> be powered by the electrical engine alone, and be charged directly off the electrical grid. For the future, advanced high capacity batteries may provide an opportunity for producing competitive long range ( $\sim 500 \text{ km}$ ) electrical vehicles (EVs).

In the exemplified fields and many more, lithium based batteries are being introduced (see Appendix). However, for widespread use there are barriers to overcome – in part technological, in part economical – depending on the specific application. Lithium batteries are the most energy dense batteries of today, but are also the most expensive. The overall cost of a battery per kWh depends on how the battery is used, for example depth of discharge and cycle life, but for a rough comparison the cost invested per kWh after the first battery cycle has been estimated to 900 USD for a lithium ion battery, compared to 300 USD for a nickel metal-hydride

battery.<sup>2</sup> As a back-up system for electrical grids, batteries have to be “dirt-cheap”, and made out of materials that you “trip over in your backyard” to provide a reasonable cost per kWh stored.<sup>3</sup> Also, for consumer electronics and transportation applications – considered high volume, but low value markets – there is an economic barrier that restricts the technologies that can be introduced. The Li-ion cell exemplified above, would have to sustain approximately 10000 cycles (~27 years if 1 cycle/day) to reach a cost of 0.15 USD (~1 SEK) / kWh,<sup>2</sup> which is well above the limit of the battery and still above the economical threshold for several applications. Thus, alternative battery technologies based on cheaper materials, such as sodium sulphur batteries,<sup>4</sup> are also being explored for large scale applications. On the other hand, for military and space applications, which are low volume but high cost markets, expensive battery technologies, can be afforded. However, these applications face more challenging technological requirements, since the batteries often need to operate under harsh conditions, in terms of temperatures and pressures.

Regardless of the area of application, the development of suitable battery technologies into commercial products is costly and investors seek to guarantee their money before the next technological leap, which identifies another obstacle in battery development – maturity time. In a recent perspective on the future of lithium battery technologies, three stages of rechargeable lithium battery development are foreseen:<sup>5</sup> in short term (0–3 years) known Li-ion battery technologies will be commercialized; in midterm (3–7 years) advanced Li-ion technologies will be introduced, based on new materials and material processing techniques that are currently being developed; in long term (7-20 years) new lithium batteries are expected to go beyond the Li-ion technology – considered a “pertinent bridge” to more advanced lithium (and non-lithium) battery technologies. An example of the very bold strategies and goals of a long term project is given by the metal-air ionic liquid (MAIL) battery project.<sup>6</sup>

Finally, a broad range of considerations exist beyond the technological and economical imperatives; battery safety and lifetime are key considerations for new applications; the toxicity and environmental benignity of individual materials relate to the safety in handling, storage, and recycling of battery components, which are not necessarily green products *per se*.<sup>7</sup> The source, abundance, and geographical location of materials, define the possibility, cost, and energy required to extract and pre-process the materials, and identify potential political risks involved. In conclusion, the development of new battery technologies is truly a multi-faceted problem.

## 2 BACKGROUND

Entitled “New anions for lithium battery electrolytes”, the central topic of this thesis is a limited part of the lithium battery. The background introduces important battery concepts, components, and materials, with the interactions between the main components as a central theme. Strategies for designing new electrolytes are highlighted, with focus on the properties of the anion.

### 2.1 Battery concepts

When two different electronically conducting materials, *electrodes*, are brought into contact, electrons flow spontaneously in the direction that cancels the electrochemical potential difference,  $\Delta\mu=E$ , of the two materials. The thermodynamic driving force is a minimization of the total free energy,  $G$ , of the system (eq. 2.1)<sup>8</sup> – here the energy available to do electric work – where  $n$  is the number of electrons transferred and  $F = 96485 \text{ C mol}^{-1}$  (Faraday’s constant) is the charge of one mole of electrons.

$$\Delta G = -nFE \quad (2.1)$$

The practical application of this process is realized in the galvanic electrochemical cell.<sup>9</sup> In the galvanic cell, direct electrode contact is avoided by positioning an ion conducting, but electronically insulating *electrolyte* between the electrodes; electrons flow between the electrodes indirectly, via an external wire to power an electronic device, while the electrolyte provides the medium for an ionic current that balances the electric current for overall charge neutrality. Batteries are strictly assemblies of several electrochemical cells, but the terms are used interchangeably.

In batteries, the electric current is sustained by coupling a suitable reduction and oxidation (redox) reaction to the electrode/electrolyte interfaces. Electron transfer occur in two half reactions – one at each electrode – coupled by the ionic mass transport through the electrolyte. The half-reaction at an electrode is characterized by a standard electrode potential,  $E^\circ$ , defined as the potential of a cell under standard conditions (1 bar, 25°C), where the electrode of interest is combined with a reference, the Standard Hydrogen Electrode (SHE).<sup>8</sup> In a cell with any two given electrodes, an estimate of the overall potential or thermodynamic driving force of the cell is given by the sum of the standard potentials, and the relative values indicate at which electrode reduction and oxidation will occur. The convention is to name the electrodes in accordance with the processes that occur in a spontaneously operating cell; reduction

occurs at the cathode, while oxidation is associated with the anode – the two can be visualized as the sink and source of electrons, respectively. In battery literature, the electrodes acting as the anode and cathode at discharge are frequently referred to as the negative and positive electrodes, respectively – irrespective of the mode of operation. A battery is usually a closed system, but in metal-air batteries, such as zinc-air<sup>10</sup> and lithium-air batteries,<sup>11</sup> air is the external reservoir of oxygen (cathode material).

### ***Performance characteristics***

From a thermodynamic driving force perspective, an optimal battery would be constructed from two electrode materials with an as large electrochemical potential difference as possible. However, in practice it is hard to find electrolytes that are chemically inert in a large electrochemical window and the cell materials must meet additional criteria. In particular, the density of active materials in each electrode is of importance for the energy density of the battery. A number of characteristics are used to rate the performance of individual components, cells, and entire batteries, for example; the specific energy (Wh/kg) or volume based energy density (Wh/dm<sup>3</sup>), the specific rated power (W/kg) or the rated power density (W/dm<sup>3</sup>). Another common characteristic is the specific capacity (Ah/kg), which states the total charge that can be delivered from a cell per unit weight of active materials. In practical batteries, independent of the cell chemistry, the energy available from the battery is estimated to be only 25-30 % of the theoretical specific energy of the active materials.<sup>10</sup> The reasons include a combination of non-active and active materials in the battery design, non-optimal contact between electrodes and electrolyte, and limited operating conditions (batteries are never fully discharged). Therefore, the engineering of batteries, for example the design of nano-structured electrode architectures, is important to increase both the ratio of active to non-active materials and the material utilization.

When no net current is delivered by the battery, it is characterized by an open-circuit potential (OCV), but the cell potential is reduced with load. The depth of discharge (DOD) expresses the delivered capacity as a percentage of the available capacity, and the discharge rate (C-rate) is a measure of the time taken to deliver the full capacity of the battery. At a 2C-rate the full capacity of the battery is discharged in half an hour (C/time (hours)). The cycle-life of the battery will depend on both the DOD and C-rate, among other factors.

### ***Rechargeable battery systems***

The status at the turn of the millennium of a few representative rechargeable (secondary) cell chemistries is summarized in Table 1. Of these, the lead-acid battery was first (1859) and accounted, in the late 90's, for more than half of the world battery sales, with its main application in vehicles for start-up, lighting, and ignition (SLI).<sup>12</sup>

**TABLE 1.** Components and practical performance of rechargeable battery systems at 20°C.<sup>10</sup>

Trivial names	Anode/Cathode	Electrolyte	V <sub>OCV</sub>	Wh kg <sup>-1</sup>	Wh dm <sup>-3</sup>
Lead-acid	Pb/PbO <sub>2</sub>	H <sub>2</sub> SO <sub>4</sub> (aq)	2.1	35	70
NiCd	Cd/NiOOH	KOH (aq)	1.3	35	100
NiMH	MH/NiOOH	KOH (aq)	1.4	75	240
Li-ion	Li <sub>x</sub> C <sub>6</sub> /Li <sub>1-x</sub> CoO <sub>2</sub>	LiPF <sub>6</sub> (non-aq)	4.1	150	400

The lead-acid battery has been followed by the nickel-cadmium (NiCd; 1899), nickel-metalhydride (NiMH; 1989), and lithium ion (Li-ion; 1991) alternatives – all competitors in the portable electronics market. Each of these cells have their advantages and disadvantages,<sup>10</sup> in Table 1 only a few basic properties are highlighted. In the comparison, Li-ion batteries stand out with an unusually high cell potential, a non-aqueous electrolyte, and the highest specific energy and energy density. The energy densities and specific energies of battery cells depend on the actual cell design and are therefore distributed around the values of Table 1.<sup>13</sup>

### ***Li-ion battery operation mechanism***

In the state-of-the-art Li-ion rechargeable battery, lithium ions are cycled between a graphite anode, Li<sub>x</sub>C<sub>6</sub>, and a lithium cobalt oxide cathode, Li<sub>1-x</sub>CoO<sub>2</sub>. The electrolyte is a liquid or gel composed of a mixture of organic carbonates with LiPF<sub>6</sub> as the Li<sup>+</sup> source. During charge and discharge, the lithium ions migrate reversibly between the anode and cathode, in a process highlighted by trivial names such as the rocking-chair<sup>13</sup> and shuttlecock<sup>14</sup> battery (Figure 1).

## **2.2 Electrodes and interfaces**

In a battery cell, the electrodes enclose the electrolyte, which has the difficult task of mediating ion transfer between two very demanding environments, while maintaining its chemical integrity. The result is an often complex interplay between the electrodes and the components of the electrolyte, a compromise in the choice of active materials, and a reliance on meta-stable battery systems. The aim of this section is to introduce common electrode materials of lithium batteries in the context of electrode/electrolyte compatibility, and to identify implications of the specific electrode materials for the choice of electrolyte.

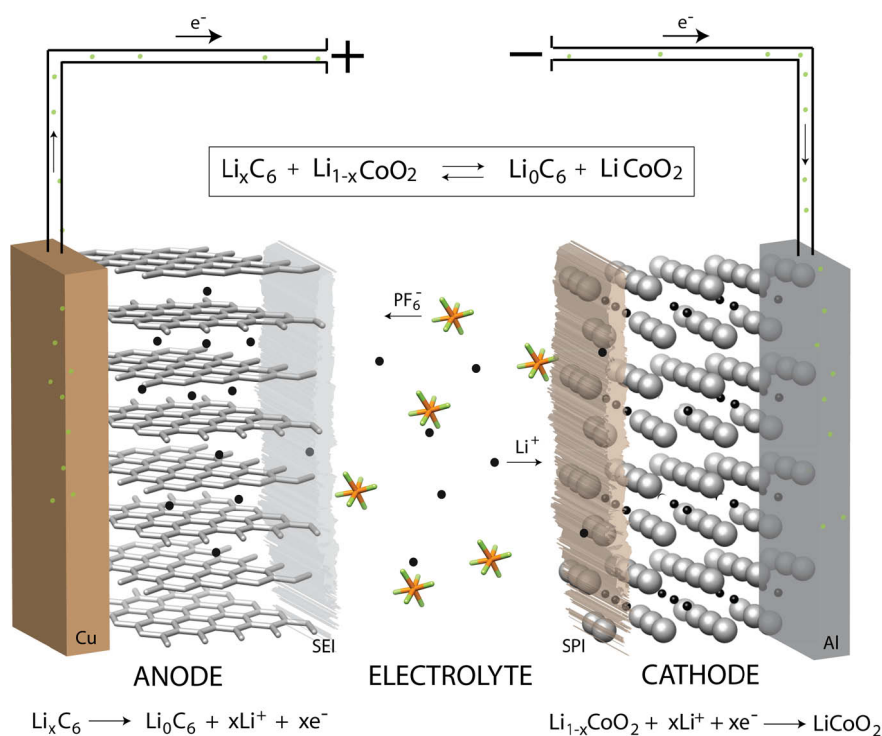


**Figure 1.** Components and discharge reactions of the state-of-the-art Li-ion cell.

### ***Anodes and the anode/electrolyte interface***

The interest in  $\text{Li}^+$  conducting electrochemical cells has its origin in two main properties of metallic lithium; the low standard reduction potential ( $\text{Li}^+ + \text{e}^- \rightleftharpoons \text{Li}$ ;  $E^\circ = -3.045 \text{ V}$ ),<sup>8</sup> and the small size of lithium ions. The first property makes lithium suitable to construct cells with large electrochemical windows, using the right cathode materials. The small size translates to a high gravimetric and volumetric density;  $0.14 \text{ mol g}^{-1}$  ( $7.69 \cdot 10^{-2} \text{ mol cm}^{-3}$ ), and a high capacity,  $3860 \text{ Ah kg}^{-1}$  ( $2060 \text{ Ah dm}^{-3}$ ).<sup>10</sup> The ion size is also important for the possibility to use intercalation electrodes.

Ideally, for a thermodynamically stable battery, the electrochemical potentials of the electrodes should be located within the stability window of the electrolyte;<sup>15</sup> no driving force should exist for electrons to transfer neither from the anode to the lowest unoccupied molecular orbitals (LUMO) of any electrolyte component, nor from the highest occupied molecular orbitals (HOMO) of the electrolyte to the cathode (Figure 2). However, if lithium metal is chosen as the anode, it will react with any electrolyte and stable cell operation will be possible only if the lithium surface is passivated by the decomposition product(s) – the formation of a solid electrolyte interphase (SEI).<sup>16</sup> The vigorous and continuous reaction of lithium with water discloses the use of an aqueous electrolyte and therefore, non-aqueous electrolytes are necessary.

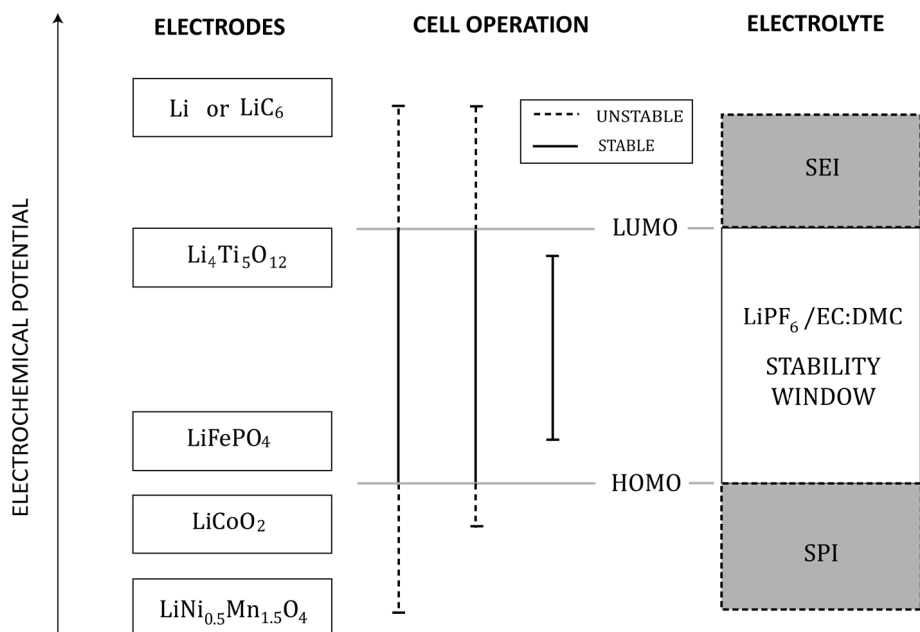


**Figure 2.** A schematic representation of the electrode/electrolyte interplay in terms of the electrochemical potential window defined by the electrodes or intrinsic to the electrolyte.

The SEI is a protective dynamical thin film, from a few to hundreds of Å thick,<sup>17</sup> that ensures a kinetically, as opposed to a thermodynamically, stable system and function as an extended electrolyte. Therefore, it should also support the migration of lithium ions and be electrically isolating. The properties of the SEI depend on the electrode, electrolyte, and the operating conditions, and have been crucial throughout the history of lithium battery development.<sup>18</sup> For lithium metal battery research, limited control over the lithium metal SEI was the root of frustration, which culminated with the unsuccessful commercialization of these batteries at the end of the 1980's.<sup>19</sup> When lithium metal batteries are charged, the plated lithium forms a rough surface at the lithium anode and an inhomogeneous SEI from electrolyte components.<sup>18</sup> The growth of tree-like structures – lithium dendrites – are observed<sup>20</sup> and attributed to the loss of active material, cell shorting,<sup>21</sup> battery explosions, and related safety incidents.<sup>13</sup> In the first successfully commercialized Li-ion batteries the problem of dendrite formation was resolved by introducing lithium intercalation compounds and topochemical reactions,<sup>22-24</sup> instead of metallic lithium and lithium plating.

The potential of lithiated graphite ( $\sim 0.05\text{V}$  vs  $\text{Li}^+/\text{Li}$ ) is almost as low as that of metallic lithium. However, a substantial trade-off is the much lower theoretical specific capacity of the graphite intercalation electrode ( $372\text{ Ah kg}^{-1}$ ) compared to a lithium metal anode ( $3860\text{ Ah kg}^{-1}$ ). A stable SEI is still needed despite avoiding dendrite formation. The SEI on graphite must be formed before  $\text{Li}^+$  intercalation, to avoid co-intercalation of electrolyte components.<sup>17</sup> In the original Li-ion battery by Sony,<sup>25-26</sup> propylene carbonate (PC) was the main component of the electrolyte, but PC co-intercalates into graphite and decomposes to propene gas that deteriorates

(exfoliates) the electrode.<sup>17</sup> A more amorphous carbon anode, petroleum coke, was then used, but later PC was substituted by ethylene carbonate (EC) and graphite could again replace petroleum coke (graphite can intercalate roughly twice the amount of lithium ions).<sup>27</sup> The SEI formation on carbon anodes is more or less completed during the first charge, with different onset potentials, better defined for graphite compared to the disordered carbons, of Li<sup>+</sup> intercalation and SEI formation.<sup>17</sup>

Beyond lithium metal and carbonaceous materials for lithium battery anodes, lithium alloys were already in the 70's able to address dendrite formation.<sup>28</sup> Lithium alloy research has focused on cheap and abundant elements, such as Si, Sn, Sb, Al, and Mg, and are attractive since their capacities fill the gap between metallic lithium and graphite, or even exceed that of metallic lithium.<sup>29</sup> The main drawback is large volume changes during cycling, detrimental to the electrode.<sup>30</sup> However, in a suitable matrix, such as carbon, this can be controlled and hundreds of cycles with good performance has been demonstrated.<sup>31</sup>

Yet another interesting class of anode materials are ceramics that avoid lithium plating by operating at a low potential; 1-2V above lithium. The best representative of this class is Li<sub>4</sub>Ti<sub>5</sub>O<sub>12</sub> (LTO),<sup>32</sup> which in combination with a LiFePO<sub>4</sub> (LFP) cathode represent a novel lithium battery approach where both the anode and cathode operate within the electrolyte stability window.<sup>33</sup> These batteries are fast-charging (5 min at 500V/125A), have long cycle life (>30000 cycles), and have recently been suggested for long term operation of city EVs and implemented in demonstration vehicles.<sup>34</sup> However, with an operating voltage of ~2V and a theoretical anode capacity limited to 175 Ah kg<sup>-1</sup>, the trade-off in energy density is substantial. For an overview and comparison of the intrinsic properties of lithium, carbonaceous, LTO vs. alloy anodes, a recent review is recommended.<sup>29</sup>

### ***Cathodes and the cathode/electrolyte interface***

The passivation need is not exclusive to the anode/electrolyte interface, as high cell voltages necessitate the use of strongly oxidizing cathodes.<sup>35</sup> Adequate stabilization of these cathodes is a main concern for the safety of lithium batteries.<sup>36</sup> Also, key differences between the surface films formed on either electrode has been observed, in particular increased thickness of cathode surface films with cycling, during storing, or elevated temperature operation. This has motivated the use of a unique term, the solid permeable interface (SPI), for the description of the cathode-electrolyte interface.<sup>35</sup>

A large number of materials have been investigated as cathodes, mainly transition metal based layered oxides (LiMO<sub>2</sub>; M=Co, Ni, Mn),<sup>37</sup> spinel type structures (LiMn<sub>2</sub>O<sub>4</sub>),<sup>38</sup> or polyanionic compounds, such as the olivine structured LiFePO<sub>4</sub>.<sup>39</sup> Also, doping with metals has been used to tune various properties; standard potentials, electric and ionic conductivity, as well as interfacial properties. In addition, surface coating and other material processing techniques have been used to control the SPI.

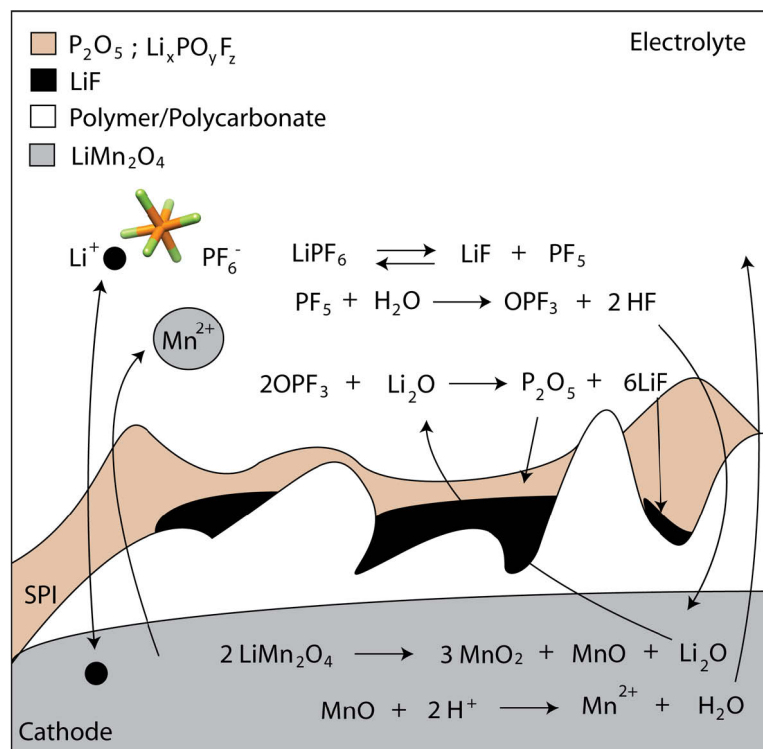


**Figure 3.** Model of the formation of a solid permeable interface between a  $\text{LiMn}_2\text{O}_4$  cathode and a  $\text{LiPF}_6$  organic liquid electrolyte. Redrawn from Edström et al.<sup>35</sup>

Detailed overviews of cathode material research, and especially doping,<sup>15</sup> are available in several recent reviews.<sup>15,40-41</sup>  $\text{LiCoO}_2$  is still, after some modifications,<sup>40</sup> the most common cathode in Li-ion batteries.<sup>41</sup> However, there are numerous concerns related to the use of  $\text{LiCoO}_2$ ,<sup>42</sup> disqualifying it for use in large scale battery applications.<sup>40</sup> Most are related to structural instability, manifested through cobalt dissolution<sup>43</sup> and loss of oxygen, when more than half of the lithium is extracted from the cathode.<sup>15</sup> As a consequence, only half of the lithium is available for the cell operation, limiting the capacity of the cathode to  $\sim 140 \text{ mAh g}^{-1}$  at a cut-off potential of  $\sim 4.2 \text{ V}$  vs.  $\text{Li}^+/\text{Li}$  (plateau  $\sim 3.7 \text{ V}$ ).<sup>44</sup> The high cost of  $\text{LiCoO}_2$  and the toxicity and rarity of cobalt, are additional concerns.

The spinel structured  $\text{LiMn}_2\text{O}_4$  played a special role in the development of the liquid electrolytes that came to dominate Li-ion batteries from the mid 90's (see below).  $\text{LiMn}_2\text{O}_4$  is considered non-toxic, cheap, and environmentally friendly ("green"), but historically oxygen release and in particular Mn dissolution, have resulted in poor cell cyclability and safety.<sup>40</sup> Now this material and doped variants are commercialized,<sup>45</sup> as a 3D  $\text{Li}^+$  diffusion offers higher rate capabilities at operating voltages similar to the 2D layered  $\text{LiCoO}_2$ .<sup>40</sup> Also, doped variants of  $\text{LiMn}_2\text{O}_4$  in combination with LTO have been suggested for 12V Li-ion batteries (5 cells à 2.5V) competitive with the lead-acid standard.<sup>46</sup>

$\text{LiFePO}_4$  is another green cathode material; elements are abundant and non-toxic and can be made at low cost, despite high processing costs for engineering of particle

size and carbon-coating.<sup>47</sup> The latter is necessary because of the poor electric conductivity, limiting the rate capability. With respect to cathode materials, LiFePO<sub>4</sub> has received overall most attention for transport applications due to thermal stability and structural integrity. The harder bound oxygen atoms and lower average operating voltage, ~3.5 V vs. Li<sup>+</sup>/Li, are advantages for cell safety. However, for the energy density the latter is a disadvantage. Also, the volumetric energy density suffers from reduced particle size and carbon coating; the packed powder density (tap density) is at best 50% of commercial LiCoO<sub>2</sub> (~2.6 g cm<sup>-3</sup>).<sup>47</sup>

### ***Anode vs. cathode electrolyte interfaces***

Several models for the formation of both SEIs and SPIs have been suggested, but there is still not a consensus about the compositions.<sup>17-18</sup> The comparison of different films are complicated by their complex dependence on several parameters; the electrodes, the electrolyte components, cell operation conditions, impurities, as well as the aging or dynamic restructuring of the films.<sup>17-18</sup> Because of the difficulties involved in predicting the composition and stability of the surface films on either electrode, the reactions involved in the formation of these films are often referred to as *ad-hoc* surface chemistry.<sup>13,48</sup> Modifications of electrode surfaces or the development of concentration gradient electrodes<sup>49</sup> are strategies used, as well as to change the electrolyte composition, either salts and/or solvents, or by adding new components (additives).<sup>50-51</sup>

## **2.3 Electrolytes**

The active chemistry at the interfaces discussed in the previous section can be considered necessary to resolve the issue of electrode/electrolyte compatibility, but at the same time it disqualifies the electrolyte from being inert. The balance in the compromise between safety and energy density in these kinetically stabilized systems is application dependent. When safe operation is the primary goal, improved electrolyte stability is needed, true especially for use with new stable high voltage cathodes. Ideally, the electrolyte should, apart from a wide EPW (Figure 2), have the following characteristics:<sup>48</sup>

- high lithium ion conductivity and low electronic conductivity over a wide temperature range.
- tolerance towards unplanned electric, mechanical, and thermal abuse, for example overcharge, crushing, or overheating.
- be composed of renewable, non-toxic, eco-friendly, and low cost materials.

More specific targets are nested with the type of application, for example transport applications.<sup>52</sup> Typical demands on ionic and electronic conductivity are  $\sigma_{ion} > 10^{-4}$  S cm<sup>-1</sup> and  $\sigma_e < 10^{-10}$  S cm<sup>-1</sup>, and a working temperature range of -20°C to +60°C.<sup>18</sup>

A high ionic conductivity,  $\sigma_{ion}$ , requires a large number,  $n_i$ , of ions (carrying a charge  $q_i$ ) with a high mobility,  $\mu_i$  (eq. 2.2). Preferentially, most of the charge should be carried by Li<sup>+</sup>, implying a high cation transport number,  $t_+$  (eq. 2.3). However, this is typically not the case; the small lithium ion is strongly solvated in the electrolyte, often with a coordination number of four (see paper IV), and drag the solvent along. This limits the cation mobility and frequently the anion dominates the charge transport. The details of transport properties of both electrodes and electrolytes have been reviewed in reference [53].

$$\sigma_{ion} = \sum_i n_i q_i \mu_i \quad (2.2)$$

$$t_+ = \frac{\mu_+}{\mu_+ + \mu_-} \quad (2.3)$$

Typical electrolyte salt concentrations are 1 to 3 mol dm<sup>-3</sup>, where the lower limit is set to prevent polarization effects, and exact values depend on an energy or power battery design and application, as well as the salt and solvent properties.<sup>54-55</sup> It is a challenge to maintain high ionic conductivity and salt solubility across a wide working temperature range. Nevertheless, practical electrolytes with ionic conductivities well above 1 mS cm<sup>-1</sup> at -60°C have been demonstrated.<sup>56</sup> In the following, three main groups of electrolyte concepts are introduced; *liquid and gel*, *solid polymer*, and *ionic liquid* electrolytes, with the aim of discussing a few strengths and weaknesses of each, important for implementation in lithium batteries. The lithium salts are treated in a separate section.

### ***Liquid and gel electrolytes***

From sections 2.1 and 2.2 it naturally follows that the development of electrodes and electrolytes is entangled. Two solvents were early used; PC was in the first commercial Li-ion batteries,<sup>25</sup> and EC, mentioned in the 1990 patent of Sony,<sup>26</sup> figured as a co-solvent to PC.<sup>57-59</sup> EC has a “high” melting point, 36.2°C,<sup>59</sup> and is therefore not suitable as a single solvent. However, in mixtures with linear carbonates, EC was identified as an indispensable component of liquid electrolytes (LE), compatible with the LiMn<sub>2</sub>O<sub>4</sub> cathode.<sup>55,60</sup> Later two ternary electrolytes were suggested; 1M LiPF<sub>6</sub> in DMC:EC (1:2 w/w) and 1.5M LiPF<sub>6</sub> in DMC:EC (2:1), after a systematic investigation of the solvents dimethyl carbonate (DMC), diethyl carbonate (DEC), diethoxyethane (DEE), EC, and PC, and a number of salts; LiAsF<sub>6</sub>, LiPF<sub>6</sub>, LiBF<sub>4</sub>, LiClO<sub>4</sub>, LiCF<sub>3</sub>SO<sub>3</sub> (LiTf), and LiN(CF<sub>3</sub>SO<sub>2</sub>)<sub>2</sub> (LiTFSI).<sup>55</sup>

A clear impact of these electrolytes was seen within a few years. In 1996, an analysis of five commercial (Sony, Sanyo, Matsushita, Moli, and A&T Battery) 18 650

type Li-ion cells indicated that EC-based carbonate mixtures dominated. Only the Sony cells still relied on PC.<sup>61</sup> The properties of liquid EC-based electrolytes are extensively summarized in reference [48].

Closely related to LEs are hybrid or gel polymer electrolytes (GPEs), where a LE is incorporated into a polymer matrix, for example a co-polymer of vinylidene difluoride and hexafluoropropylene P(VdF-HFP).<sup>62</sup> GPEs offer advantages in terms of cell flexibility and cell design according to the “Bellcore-concept”,<sup>63</sup> where three laminated cell parts (anode + Cu-current collector, electrolyte, and cathode + Al-current collector) are fused together. Here a non-active plasticizer is used as a temporary, later extracted, stand in for the moisture sensitive LE, leaving a porous laminate, which in a subsequent dry activation step is filled with the LE. Li-ion cells constructed in this way are known as plastic Li-ion (PLiON). Apart from a flexible design, the “all” plastic design of the PLiON batteries offers an energy density advantage over the ordinary Li-ion cells with a metal casing. However, since they share the same active materials as Li-ion cells, they operate in the same way, with similar operational benefits and drawbacks. In newer generations of GPEs, which have required the trivial name Li-ion polymer batteries, the P(VdF-HFP) matrix have been replaced by a gel-coated poly-olefin separator.<sup>13</sup>

Irrespective of the liquid or gel nature of the electrolytes discussed above, their most important shortcomings are attributed to the organic solvent components; high flammability and low flashpoints, and often restricted to operating temperatures above - 20°C, owing to the presence of EC. There is also the mismatch in EPW towards common electrodes (Figure 2).

### ***Solid polymer electrolytes***

Contrary to GPEs, which contain organic solvents, the concept of using a polymer as the sole electrolyte solvent impose different electrochemical properties to the overall lithium battery. The most important is the possibility to combine the solid polymer electrolyte (SPE) with a lithium metal anode, since the corresponding interface is more mechanically resistant to dendrite growth (section 2.2). In principle, this leads to a more reliable cell with a higher energy density – “perfectly suitable for electrical vehicle application”,<sup>64</sup> and alternative large scale battery applications.

The initial interest in SPEs<sup>65</sup> in the late 1970’s was inspired by the favourable alkali ion/polymer interactions that had been observed in poly(ethylene oxide) (PEO)<sup>66</sup> and the low reactivity of the ether (–C–O–) linkage.<sup>67</sup> Consequently, the first constructed lithium polymer battery (LPB)<sup>68</sup> in the early 1980’s used a PEO-based electrolyte, but operated at temperatures > 120°C, which highlights one of the inherent problems of these electrolytes – poor room temperature ionic conductivity. The ionic conductivity of PEO lithium salt complexes is commonly of the order  $10^{-6}$  -  $10^{-8}$  S cm<sup>-1</sup> at room temperature,<sup>67,69</sup> with the exception of the use of a plasticizing lithium salt (LiTFSI/PEO,  $\sigma_{\text{ion}} \sim 10^{-5}$  S cm<sup>-1</sup>).

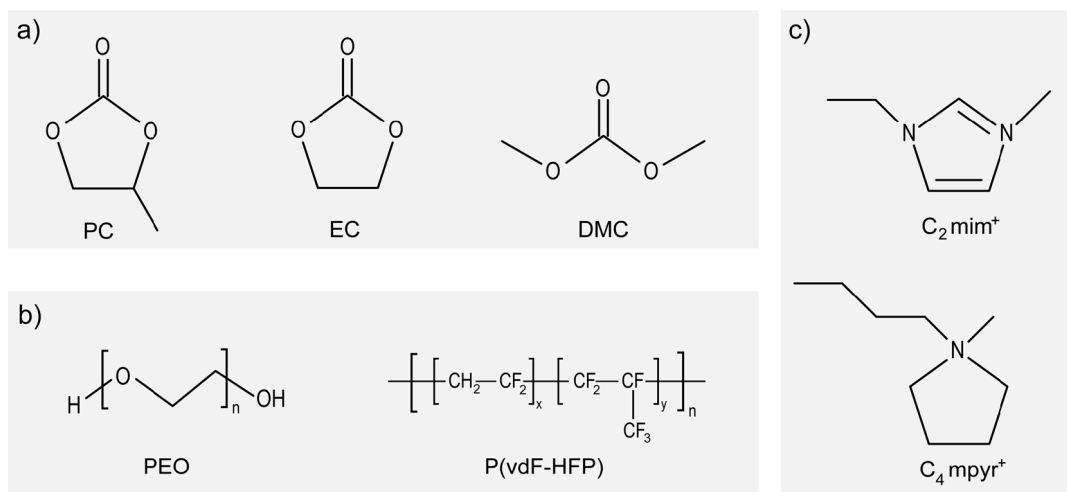


**Figure 4.** Solvent components used or considered for use in lithium battery electrolytes; a) organic liquids, b) polymers, c) IL cations.

With the facile ion transport occurring in the amorphous phase, the high crystallinity of PEO was early identified as the main hurdle to facile ion transport. Therefore, various attempts have been made to replace or modify PEO. However, it has been proven difficult to find a more suitable polymer than PEO that combine high ionic conductivity with mechanical and electrochemical stability.<sup>70</sup> Instead, the addition of ceramic fillers, forming composite polymer electrolytes (CPEs), have shown favourable effects on both ion transport properties and interface stability.<sup>67,70-73</sup> However, control over particle size, sample uniformity, and reproducibility has proven a challenge.<sup>73</sup> Nevertheless, the development of CPEs has led to batteries competitive for electric vehicle applications.<sup>74</sup>

Concluding this section, two out-of-the-box examples of polymer electrolytes are mentioned. In the first, the polymer-in-salt electrolyte,<sup>75</sup> the concept of a SPE is reversed, with for example 15% PEO (w/w) in a lithium salt. The second example, the polymer in ceramic electrolyte,<sup>76</sup> follows a corresponding approach, where a porous ceramic phase acts as a matrix for a liquid oligomer and a lithium salt. The aim of both these approaches is to combine the good transport properties of alternative glassy and ceramic solid-state electrolytes,<sup>69</sup> which suffer from brittleness and mechanical rigidity, with the flexibility and surface adhesive properties of polymers.

### ***Ionic liquid based electrolytes***

One of the simplest imaginable electrolytes is an ionic system free of solvent, where a single salt provides the charge carriers as well as the medium for ion transport. For lithium batteries such an electrolyte would be realized by a lithium salt, molten over the operating temperatures of interest – a Li<sup>+</sup> based ionic liquid (IL).

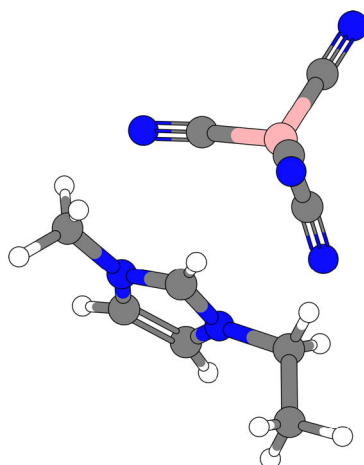


**Figure 5.** Geometry of an ion-pair of the ionic liquid  $C_2mim[B(CN)_4]$ . Bulky and dissimilar ions are responsible for the low melting points of ionic liquids.

However, a molten lithium salt is hard to realize at moderate temperatures, and therefore the simplest IL based electrolytes are ternary systems, resulting from a lithium salt and an IL sharing the same anion.

A popular definition of an IL is “a salt with a melting temperature below  $100^\circ C$ ”, which is possible for ionic systems where crystallization is hindered by a combination of certain ion characteristics; low surface charge, large size, low symmetry, conformational flexibility, and inter-ionic mismatch (Figure 5).<sup>77-78</sup> The strict requirements on the battery electrolyte drastically reduce the number of potentially useful ILs, but there exist ILs that fulfil electrode compatibility, high ionic conductivity, and a wide liquid temperature range etc.<sup>78</sup> The implementation of ILs as solvents for lithium batteries is foremost driven by expectations of improved battery safety, as a result of several intrinsic properties of ILs, such as their low volatility, low flammability, and electrochemical stability.

Among the disadvantages are cost and high viscosities,<sup>79</sup> the latter generally increasing when a lithium salt is added. The former is believed to restrict the use of ILs as solvents for any cost-sensitive application,<sup>80</sup> such as transportation and grid storage. Recent studies have also revealed onset temperatures for thermal IL decomposition lower than first reported<sup>80-81</sup> and addressed the chemical instability of ILs.<sup>81</sup> Moreover, tests of Li-ion cells have shown similar behaviour for IL and carbonate based electrolytes, in the event of thermal runaways.<sup>82</sup> However, differences in onset temperatures and the amount of heat generated do exist, in particular as a function of the anion. A similar anion dependence has been observed for ILs heated in the presence of charged electrode surfaces.<sup>82-83</sup>

An interesting alternative to neat ILs are ILs incorporated in polymer electrolytes,<sup>78,84-85</sup> yet another is combinations of ILs and organic solvents, which might seem counter-intuitive. However, the objective is to improve the interfacial<sup>86</sup> and transport<sup>87-88</sup> properties of the neat IL based electrolytes, without compromising the

thermal properties. The possibility of including organic solvents in additive amounts to implement a lithium metal anode has been addressed,<sup>86,89</sup> and the required passivation shown to depend on both the IL constituents and lithium salt.<sup>90-92</sup>

## 2.4 Lithium salts

A lithium salt, or several, has to be added to a solvent, or more often several, to provide a  $\text{Li}^+$  conducting electrolyte with a high enough concentration of charge carriers (section 2.3). As also mentioned in the previous section, no two-component  $\text{Li}^+$  ILs are available, implying that a minimum of three components are required for an  $\text{Li}^+$  conducting electrolyte. An exception is the use of anion functionalized polymers, or polymer/salt hybrids, where one or both of the polymers chain ends are modified by attaching a negatively charged group that coordinates  $\text{Li}^+$ .<sup>77</sup> Thus, the salt and solvent are the same.

To find an optimal counter-ion to  $\text{Li}^+$  is far from trivial. The interactions of the anion with  $\text{Li}^+$ , solvent molecules, electrodes, and even the current collectors, pose the same difficulties choosing a suitable counter-ion, as a solvent or solvent mixture. A substantial number of requirements have to be fulfilled simultaneously for an electrolyte, and it can be very challenging to substitute any single component. This is perhaps the main reason why so little progress has been made in the area of new lithium salts, despite the well-known drawbacks of the state-of-the-art lithium salt: lithium hexafluorophosphate ( $\text{LiPF}_6$ ). Chosen for the pioneering Sony Li-ion cell, it is still, almost exclusively, implemented in modern Li-ion batteries, as part of LEs or GPEs.

In the following sub-sections several properties of  $\text{LiPF}_6$  are reviewed together with early competitor salts. The main disadvantage of  $\text{LiPF}_6$ , its thermal instability, is discussed separately, followed by a section devoted to the introduction of alternative salts. These salts represent a subjective choice of research directions currently explored, to identify new alternatives for the future.

### ***Classic lithium salts***

When  $\text{LiPF}_6$  was chosen by Sony in the early 90's, it was somewhat of a surprise, since the purity of  $\text{LiPF}_6$  had not been adequate for stable, long term battery operation, in contrast to the use of  $\text{LiAsF}_6$ .<sup>19</sup> From the initial patent,<sup>26</sup> the competitor lithium salts at the time were:  $\text{LiClO}_4$ ,  $\text{LiAsF}_6$ ,  $\text{LiBF}_4$ ,  $\text{LiB}(\text{C}_6\text{H}_5)_4$ ,  $\text{LiCl}$ ,  $\text{LiBr}$ ,  $\text{Li}(\text{CH}_3\text{SO}_3)$ , and  $\text{Li}(\text{CF}_3\text{SO}_3)$  ( $\text{LiTf}$ ). In 1991, Dudley et al. (Moli Energy) used the fluorinated salts above and  $\text{LiN}(\text{SO}_2\text{CF}_3)_2$  ( $\text{LiTFSI}$ ) – a total of five lithium salts and 27 organic solvents – in the preparation and characterization of the conductivity of 150 electrolytes.<sup>56</sup> Three of these can be visualized in Figure 6. Most attention was clearly devoted to  $\text{LiAsF}_6$ , as part of 130 electrolytes. All electrolytes were composed of a single salt, but in solutions containing up to four different solvents.

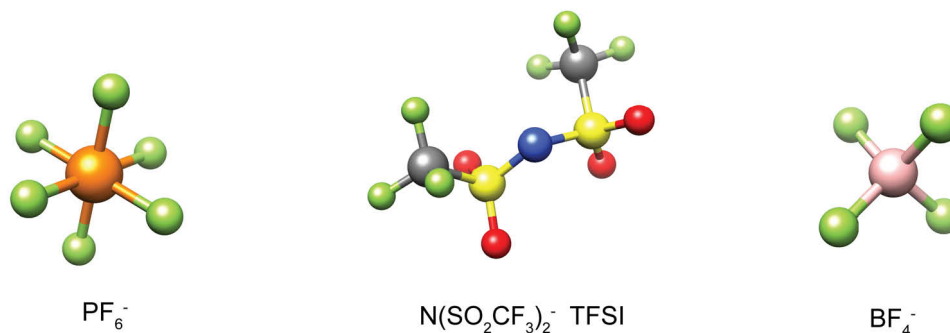


**Figure 6.** Anions of classic lithium salts.

Although the highest conductivities overall were found among the optimized  $\text{LiAsF}_6$  electrolytes, conductivity results of electrolytes on the same footing, 1M  $\text{LiX}/\text{EC}:\text{PC}$  (1:1), demonstrated the excellent conductivity of  $\text{LiPF}_6$  in carbonate electrolytes.



Mentioned in previous section, Tarascon et al. (Bellcore; 1994) used the same five salts (+ $\text{LiClO}_4$ ) in the optimization of electrolytes, based on solvent mixtures of cyclic and linear carbonates.<sup>55</sup> The results, after optimizing the electrolyte composition with respect to both ion conductivity and electrochemical stability towards a  $\text{Mn}_2\text{O}_4$  cathode, again highlighted  $\text{LiPF}_6$  electrolytes as the optimal choice. Although, these authors used  $\text{LiClO}_4$  in their study, they conveyed with the opinion of Dudley et al., and most of the battery community,<sup>56</sup> that for practical battery systems there is too much of a risk of violent reactions, due to peroxides formed from perchlorate ( $\text{ClO}_4^-$ ) decomposition. Thus, all the relevant lithium salts at the time were either inorganic high symmetry fluorinated anions,  $\text{LiTf}$  or  $\text{LiTFSI}$ . Important, is that  $\text{LiPF}_6$  and the other inorganic fluorinated salts were not suitable alternatives for SPEs, because of the vulnerability of the PEO chains to attack by the Lewis acids ( $\text{AsF}_5$ ,  $\text{PF}_5$ , and  $\text{BF}_3$ ) in equilibrium with the corresponding anions.<sup>64</sup> Thus, SPEs had been limited to the perfluorinated organic anions,  $\text{LiTf}$  and  $\text{LiTFSI}$ . Out of these,  $\text{LiTFSI}$  had become the salt of choice for SPEs.<sup>93</sup>

The success of  $\text{LiPF}_6$  can be attributed to a favourable balance of properties.<sup>48</sup> In Table 2, the electrochemical stabilities and conductivities are collected for the classic lithium salts,<sup>55</sup> together with thermal stabilities and aluminium current collector compatibilities. While  $\text{LiPF}_6$  based electrolytes have favourable high conductivity and electrochemical stability, they suffer from a lower than average thermal stability.  $\text{LiTFSI}$ , and a few analogues, labelled as indefinitely stable at elevated temperatures ( $100^\circ\text{C}$ ),<sup>94</sup> were shown to have an Achilles heel of their own – corrosion of the aluminium current collector.

**TABLE 2.** Properties of liquid electrolytes as a function of lithium salt.

Salt	1M EC:DMC (1:1) <sup>55</sup>		Non-specific <sup>48</sup>	
	E <sub>OX</sub> / V vs. Li <sup>+</sup> /Li	σ <sub>20°C</sub> / mS cm <sup>-1</sup>	T <sub>decomp</sub> / °C	Al <sub>corr</sub>
LiAsF <sub>6</sub>	4.7	11.2	>100	-
LiPF <sub>6</sub>	>5.1	11.0	~80	-
LiBF <sub>4</sub>	>5.1	5.5	>100	-
LiTf	3.2	3.0	>100	x
LiTFSI	4.4	8.0	>100	x
LiClO <sub>4</sub>	>5.1	8.5	>100	x <sup>95</sup>

### ***Thermal stability of LiPF<sub>6</sub>-electrolytes***

The thermal disadvantage of LiPF<sub>6</sub> is related to the poor chemical stability of the anion, which is slowly degraded even at ambient temperatures. The degradation rate increase with temperature, especially when catalyzed by impurities or electrode materials, and already at temperatures >60°C the negative effects on the performance of LiPF<sub>6</sub> based cells are severe.<sup>96</sup> After a few days of heating at slightly higher temperatures (≥85°C), the decomposition can be severe.<sup>97</sup> Two main safety risks identified with these reactions are; the possibility of explosions, due to the formation of gaseous products and increased cell pressure, and health concerns associated with the high toxicity of several proposed fluorinated decomposition products.<sup>98</sup>

In solid LiPF<sub>6</sub>, there is an unavoidable equilibrium between the salt and the Lewis acid, PF<sub>5</sub> (g) (eq. 2.4); a reaction that is modified to produce OPF<sub>3</sub> (eq. 2.5) in the presence of protic impurities, such as water or alcohols.<sup>99</sup>



Among several decomposition products,<sup>99-100</sup> PF<sub>5</sub> and OPF<sub>3</sub> were identified, after several days of electrolyte storage at elevated temperatures (70-85°C). Via deliberate addition of small amounts of PF<sub>5</sub>, OPF<sub>3</sub>, or ethanol to LiPF<sub>6</sub> electrolytes, Campion et al. suggested several decomposition mechanisms in carbonate based LiPF<sub>6</sub> electrolytes and proposed that PF<sub>5</sub> is the source of OPF<sub>3</sub>.<sup>100</sup> OPF<sub>3</sub> is believed to induce continued electrolyte breakdown, triggering the formation of alkyl fluorides (R-F) and organophosphorous (OPF<sub>2</sub>OR) compounds.<sup>100</sup> As suggested by Sloop et al.,<sup>97</sup> the consumption of PF<sub>5</sub> in the electrolyte solutions implies that the anion-Lewis acid equilibrium is pushed to the right (Le Chatelier's principle), promoting continued anion breakdown. However, according to these authors, PF<sub>5</sub> was consumed through a

different route, by catalyzing EC ring opening and the formation of PEO-like polymers and CO<sub>2</sub> release.

Overall, the decomposition events in LiPF<sub>6</sub> electrolytes in the absence of electrodes are controversial, since the results of different studies can be influenced by different levels of impurities (HF, H<sub>2</sub>O, and possibly alcohols) that are unavoidably present. Only recently has a “global scheme” of thermal and electrochemical decomposition of LiPF<sub>6</sub>, DMC, and EC been presented,<sup>101</sup> where the initial steps of salt decomposition agree with those predicted by Campion et al.

The present commercial recipe for preventing thermal battery failures is to add a large number of role-assigned additives<sup>51</sup> to the electrolyte, and by implementing external safety devices. However, the alternative route of new solvents and/or salts is important, in order to create intrinsically safer electrolytes and batteries. Ideally, this will decrease the number of components in the electrolytes and the need for external safety engineering, and hopefully give Li-ion technology a push forward.

### ***Alternative lithium salts***

To compete with LiPF<sub>6</sub>, alternative salts have to offer improved thermal stability, without sacrificing too much in the other performance parameters. Returning to Table 2, the most important parameters can be identified as the electrochemical stability, ionic conductivity, and the ability to passivate the aluminium current collector. In the review by Xu,<sup>48</sup> a number of new lithium salts were listed and sorted into six families. A few of these are included here, together with newer salts developed. Six representative anions of these salts are illustrated in Figure 7.

### ***LITHIUM BORATES AND PHOSPHATES***

From the mid 90's, anions were developed based on a four-coordinated boron centre, directly bonded to oxygen atoms of larger aromatic or non-aromatic structures. Lithium bis(oxalato)borate (LiBOB)<sup>102</sup> seemed to have all the qualities needed to replace LiPF<sub>6</sub>;<sup>48,102</sup> a reported conductivity of 7.5 mS cm<sup>-1</sup> in EC:DMC, an oxidative stability up to 4.3 V vs. Li<sup>+</sup>/Li, the ability to form an SEI and SPI, and good passivation of the Al-current collector up to 6.0 V vs. Li<sup>+</sup>/Li. However, it was later concluded that organic carbonate electrolytes based on LiBOB formed a much more resistive interface, had lower salt solubility and ion conductivity, which resulted in poor low temperature performance.<sup>103-104</sup> Instead of replacing LiPF<sub>6</sub>, LiBOB rapidly assumed the role as a multifunctional additive in state-of-the-art electrolytes.<sup>50</sup> Attempts to reintroduce LiBOB as the main charge carrier salt has involved the screening for more suitable solvents<sup>105</sup> and implementation of alternative electrodes.<sup>106</sup> A modification of LiBOB to resolve the poor solubility and resistive interface is lithium difluoro(oxalato)borate (LiDFOB).<sup>107-108</sup> LiDFOB is a combination or hybrid salt of the classic LiBF<sub>4</sub> and LiBOB, and is proposed to combine the advantages of each; the good low temperature performance of LiBF<sub>4</sub> and the high temperature performance of

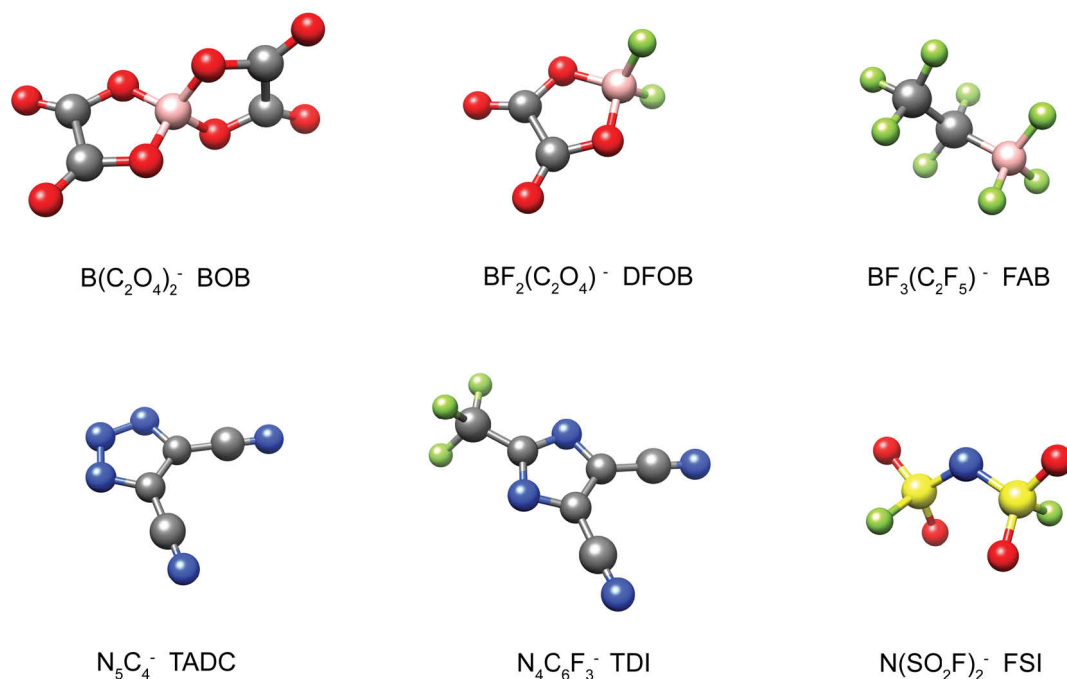


**Figure 7.** Representative anions of alternative lithium salts.

LiBOB. LiDFOB is currently under investigation in several laboratories, as the main charge carrier salt<sup>109-111</sup> or as one of two components in salt blends.<sup>112-113</sup> Parallel to the research on the LiBOB/LiDFOB couple, phosphor-based analogues have been developed, lithium tris(oxalato)phosphate (LiTOP)<sup>114-115</sup> and lithium tetrafluoro-oxalatophosphate,<sup>116-117</sup> but these salts have received considerably less attention.

Another class of hybrid lithium salts are the fluoroalkylated variants of the classic  $PF_6^-$  and  $BF_4^-$ ; the trifluoromethyl modified lithium salts,  $LiPF_{6-n}(CF_3)_n$  introduced by Kita et al.,<sup>118</sup> the lithium fluoroalkylphosphate  $Li[(C_2F_5)_3PF_3]$  (LiFAP)<sup>119</sup> developed by Merck, and the lithium fluoroalkylborates  $Li[(C_nF_{2n+1})BF_3]$ <sup>120</sup> from Mitsubishi Chemicals. The main intention with the introduction of fluoroalkyl groups was to increase the stability of the remaining P–F or B–F bonds, and thereby the thermal stability of the electrolytes. For the borates, also increased ion conductivity was a target. LiFAP/EC:DMC electrolytes were found to be slightly less conductive compared to those of  $LiPF_6$ , however, the LiFAP electrolyte showed better discharge capacity in a Li/ $Mn_2O_4$  cell, which was suggested to be a result of the improved chemical stability of FAP.<sup>119</sup> Also, in a subsequent study, favourable film formation on graphite and  $Mn_2O_4$  surfaces was attributed to less HF in the LiFAP electrolytes.<sup>121</sup> Initial electrochemical characterization of the direct borate analogue,  $Li[(C_2F_5)BF_3]$  (LiFAB), showed good discharge and cycle performance of LiFAB/EC:EMC electrolytes in Li-ion cells with a Ni-based cathode,<sup>122</sup> but further studies revealed that the performance after elevated temperature storage was poor.<sup>123</sup> This performance deterioration was attributed to a lower anodic stability of LiFAB against  $LiCoO_2$ , compared to  $LiBF_4$  and  $LiPF_6$ .

Hence, the > 5V oxidation stability measured at the surface of a Pt-electrode<sup>122</sup> did not reflect the stability against the LiCoO<sub>2</sub> surface, which is a recurring point for many electrolytes.<sup>48</sup>

#### LITHIUM METHIDE AND IMIDES

LiTFSI has been an attractive, structurally very different alternative to LiPF<sub>6</sub>. However, in liquid electrolytes, its application has been hindered by corrosion of the Al current collector (Table 2). Very early, a lithium methide salt, Li[C(SO<sub>2</sub>C<sub>2</sub>F<sub>5</sub>)<sub>3</sub>],<sup>94</sup> was suggested as an alternative to resolve the corrosion problem. Although the onset voltage for aluminium corrosion was increased (~4.5 V vs. Li),<sup>124</sup> it remained a problem for the use of high voltage cathodes. Similar results were obtained for several lithium imides with extended fluoroalkyl chains, for example the symmetric Li[N(SO<sub>2</sub>C<sub>2</sub>F<sub>5</sub>)<sub>2</sub>] “beti”,<sup>125</sup> and the asymmetric Li[N(SO<sub>2</sub>CF<sub>3</sub>)(SO<sub>2</sub>C<sub>4</sub>F<sub>9</sub>)].<sup>125-127</sup> New and extended variants of LiTFSI continue to attract interest exemplified by the recent lithium (fluorosulfonyl) (nonafluorobutanesulfonyl)imide, Li[N(SO<sub>2</sub>F)(SO<sub>2</sub>-n-C<sub>4</sub>F<sub>9</sub>)] (LiFNSFI).<sup>128</sup> However, the increased anion size affects the ionic conductivity negatively, and the high cost of large LiTFSI alternatives have been addressed before.<sup>127</sup>

In LiFNSFI, one of the trifluoromethyl groups of LiTFSI is substituted by a fluorine atom; if two fluorine atoms are substituted for both trifluoromethyl groups of TFSI, the bis(fluorosulfonyl)imide anion, N(SO<sub>2</sub>F)<sub>2</sub><sup>-</sup> (FSI) is obtained. This anion has been known in the form of several alkali salts since the 1960's,<sup>129</sup> but the potential use of its lithium salt for battery electrolytes was first recognized in the mid 90's.<sup>130</sup> In the extensive review by Xu (2004),<sup>48</sup> there was no mention of LiFSI, reflecting the anonymous first decade of this salt, following its patent disclosure.<sup>130</sup> LiFSI is smaller and lighter compared to LiTFSI, and based on the observation of suppressed Al-corrosion with an increase of the fluoroalkyl group(s), LiFSI would appear to be a step in the wrong direction. Abouimrane et al. observed a low (3.3V) onset potential for Al-corrosion by an LiFSI/EC:DMC electrolyte, but were hesitant to whether the corrosion could have been caused by Cl<sup>-</sup> contaminants.<sup>131</sup> This hypothesis was addressed by Han et al.<sup>132</sup> who added Cl<sup>-</sup> to high purity LiFSI electrolytes. They observed a corrosion current at 3.6 V, also without Cl<sup>-</sup>, but for the latter the corrosion diminished at subsequent cycles. A high purity LiFSI salt could thus resolve the problem of aluminium corrosion. In the same study, favourable cell performance was demonstrated compared to LiPF<sub>6</sub> cells.<sup>132</sup> Apart from the potential application of LiFSI in carbonate electrolytes, FSI has become fully embraced as a component of ILs, since it forms ILs with low viscosity and high ionic conductivity.<sup>133</sup> Moreover, several novel features for IL based Li-ion cells have been attributed to the anion, for example the compatibility of FSI-based ILs<sup>134</sup> (or IL mixtures)<sup>135</sup> with a graphite anode, and the possibility of uniform and reversible plating of lithium at a lithium metal anode.<sup>92</sup> This last feature is interesting for the possible application of FSI ILs in lithium metal batteries.

Overall, the features of LiFSI electrolytes are very interesting and have singled out FSI as one of the most promising replacements for  $\text{PF}_6^-$ , at present. However, there are concerns about the thermal properties – especially in the presence of trace moisture.<sup>136</sup> Huang et al. observed signs of exothermic decomposition of dry LiFSI at 183°C, which in the presence of water could occur at ~120°C, with accentuated heat release. Another important thermal aspect is the very high self-heating rates of LiFSI electrolytes,<sup>137</sup> which together with an exceptionally high amount released heat<sup>83</sup> are clear disadvantages in case of cell failure.

#### *HETEROCYCLIC CYANO BASED LITHIUM SALTS*

These anions all combine an aromatic ring structure with cyano groups for charge delocalization. The first example is the lithium dicyanotriazolate (LiDCTA or LiTADC), which was intended for SPEs.<sup>138</sup> In PEO, LiDCTA turned out to have a good plasticizing effect, although not as good as LiTFSI, and showed an improved lithium transference number compared to traditional SPEs. After the initial report LiDCTA received some theoretical interest,<sup>139</sup> but very little has been reported about this system since its first description. However, it has inspired the synthesis of related lithium salts, exemplified by the lithium 4,5-dicyano-(2-trifluoromethyl)imidazolid (LiTDI),<sup>140-142</sup> and highlighted the possibility of introducing cyano groups as electron withdrawing groups in place of fluorine atoms or fluoroalkyl groups. LiDCTA can also be considered the seed for the scientific work presented in this thesis, where cyano groups have been incorporated into most of the anion classes presented.

## **2.5 Scope of thesis**

The background of this thesis has almost exclusively been devoted to experimental properties of lithium batteries, addressing the problems encountered when choosing and assembling the core components of the battery; from the choice of electrodes (lithium metal or intercalation anodes, transition metal oxide or phosphate cathodes, effects of transition metal doping), electrolyte concepts (liquid, gel, polymer, ionic liquid, or mixtures thereof), to the choice of anion for the lithium salt (inorganic/organic, fluorinated/non-fluorinated). Also the compatibility of different components has been highlighted.

In this context it may seem absurd to address a few properties of naked (non-solvated) anions or small ion associates by means of computational modelling, and relate the results to the properties of anions and lithium salts in real, very much more complicated, electrolyte environments. However, it is also an advantage to focus on single components, without the interference of impurities, and to sequentially introduce and study the effects of minor structural modifications or added components. Also, the properties of novel systems can be predicted, even though they are not experimentally available.

This said, the central approach taken in this work is to investigate the functional group (-F, -CF<sub>3</sub>, -C≡N) dependence on the electrochemical stability of novel and existing anions, and the type and strength of anion-lithium ion interactions expected in real electrolytes. The calculated electrochemical stabilities represent intrinsic oxidation limits of the anions,<sup>143-144</sup> for which no experimental counterpart is offered. This is contrasted by the predicted ion-ion interactions, which are related to experimental systems through a comparison of computed and experimental vibration spectra, when possible. An underlying hypothesis for the study of the cyano substituted lithium salts is that the replacement of fluoro substituents will lead to more thermally stable lithium salts. The observation that LiTDI passivates aluminum at potentials < 4.6 V vs. Li<sup>+</sup>/Li is a promising sign.

Hopefully, the work of this thesis will be of use in addressing the role of the anion in future experimental work on electrolytes and lithium batteries based on the salts investigated herein. Moreover, it could be of advantage to more clearly differentiate the intrinsic properties of the anions from properties resulting due to specific environments, so that the complete electrolyte can be optimized in the best possible way.

## 3 METHODS

This thesis focuses on computationally predicting and spectroscopically corroborating properties of anions for lithium battery electrolytes. Ideally, a quick and efficient *a priori* computational screening for suitable lithium salts saves resources, by limiting costly and time-consuming material synthesis. However, the results have to be carefully interpreted with respect to the choice of model and computational method.

The first section gives an introduction to the electronic structure methods used. In the subsequent section, a background to Raman spectroscopy is provided, being the main complementary tool used for the experimental studies. Introductions to dielectric spectroscopy, differential scanning calorimetry, and electrochemical characterization, which have only been used in connection with paper V, are omitted. Descriptions of the specific setups are referred to the experimental section of that paper.

### 3.1 Computations

*Ab initio* or electronic structure methods are two common terms used to describe a number of computational approaches that, based on a quantum mechanical description of the electron distributions, are used to predict the properties of atoms, molecules, and assemblies thereof.<sup>145-146</sup> For a discussion of these methods, the time-independent Schrödinger equation and the components of the Hamiltonian operator,  $\hat{H}$ , represent a convenient starting point (eq. 3.1).

$$\hat{H}\Psi_k(\mathbf{R}, \mathbf{r}) = E_k\Psi_k(\mathbf{R}, \mathbf{r}) \quad (3.1)$$

$$\hat{H} = \hat{h}_N + \hat{h}_e = [\hat{T}_N + \hat{V}_{NN}] + [\hat{T}_e + \hat{V}_{ee} + \hat{V}_{Ne}] = \quad (3.2)$$

$$= \left[ -\frac{1}{2} \sum_{I=1}^N \frac{\nabla_I^2}{M_I} + \sum_{I=1}^N \sum_{J \neq I}^N \frac{Z_I Z_J}{|\mathbf{R}_I - \mathbf{R}_J|} \right] + \left[ -\frac{1}{2} \sum_{i=1}^n \nabla_i^2 + \sum_{i=1}^n \sum_{j \neq i}^n \frac{1}{|\mathbf{r}_i - \mathbf{r}_j|} - \sum_{I=1}^N \sum_{i=1}^n \frac{Z_I}{|\mathbf{R}_I - \mathbf{r}_i|} \right]$$

For a molecular system with  $N$  nuclei and  $n$  electrons, the Hamiltonian contains the minimum of terms presented in (eq. 3.2). When the Hamiltonian operates on a wavefunction  $\Psi_k(\mathbf{R}, \mathbf{r})$ , representing a molecular system in state  $k$  (with nuclei and electrons with coordinates,  $\mathbf{R}_I=(\mathbf{R}_{1,} \mathbf{R}_{2,}, \dots, \mathbf{R}_N)$  and  $\mathbf{r}_i=(\mathbf{r}_{1,} \mathbf{r}_{2,}, \dots, \mathbf{r}_n)$ , respectively), the terms of the Hamiltonian extract; the kinetic and potential energy of the interacting nuclei,

$\hat{h}_N$ , and the kinetic and potential energy of electrons interacting with each other and the nuclei,  $\hat{h}_e$ . Thus,  $E_k$  is the total energy of the system in state  $k$ . However, implemented for a system of three particles or more, eq. 3.1 is not analytically solvable with the given Hamiltonian, because of the dynamic inter-particle interactions. Therefore, both the Hamiltonian and wave function need to be cast in approximate forms.

In the Born-Oppenheimer approximation,<sup>147</sup> a separation of the nuclei and electron part is made, with the electron arrangement now optimized with respect to a frozen nuclear configuration (eq. 3.3). Hence, for a given nuclear configuration the Hamiltonian is reduced to the electronic part,  $\hat{h}_e$ , of equation (eq. 3.2), with one analytically non-solvable term; the electron-electron potential.

$$\hat{h}_e \Phi_k(\mathbf{r}) = \varepsilon_k \Phi_k(\mathbf{r}) \quad (3.3)$$

Somewhat simplified, the available electronic structure methods represent different approximate approaches to deal with the electron-electron interaction term, which embeds two types of interactions; 1) a repulsive coulomb interaction, due to the negative charge of the electron (*correlation*), and 2) a repulsive interaction between electrons of equal spin (*exchange*). A more general and alternative division of computational strategies refer to the direct use of Schrödinger's wavefunction formalism or an indirect density functional approach based on the squared wave function – the *electron density*. Different acronyms, such as HF, MP2, B3LYP, and VSXC, discriminate between different approaches, with respect to the specific theory and assumptions.

### **Wavefunction methods**

The Hartree-Fock (HF) approach is the fundamental wavefunction method, described as an exact-exchange/no-correlation approach; the electron exchange repulsion is fully accounted for by the implementation of an antisymmetric wavefunction, but a mean-field interaction of each electron with the average charge of the remaining electrons substitute realistic correlation effects. A detailed derivation of the general and more specific HF equations can be found in a review of the HF theory.<sup>147</sup>

In short, one way to derive the HF equations is from the variational theorem (eq. 3.4-3.5). An important implication of this theorem is that the unknown energy,  $\varepsilon_0$ , of the electronic ground-state,  $\Phi_0$ , can be iteratively approached in a process known as a *self-consistent field* (SCF) calculation. The calculation is initiated with a trial wavefunction, which is sequentially updated to minimize the system energy. A self-consistent or converged solution is obtained when the difference of two consecutive solutions becomes arbitrarily small.

$$\int \Phi_k^*(\mathbf{r}) \hat{h}_e \Phi_k(\mathbf{r}) = \varepsilon_k \int \Phi_k^*(\mathbf{r}) \Phi_k(\mathbf{r})$$

$$\Leftrightarrow$$

$$\langle \Phi_k^* | \hat{h}_e | \Phi_k \rangle = \varepsilon_k \langle \Phi_k^* | \Phi_k \rangle \quad (3.4)$$

$$\frac{\langle \Phi_k^* | \hat{h}_e | \Phi_k \rangle}{\langle \Phi_k^* | \Phi_k \rangle} = \varepsilon_k \geq \varepsilon_0 = \frac{\langle \Phi_0^* | \hat{h}_e | \Phi_0 \rangle}{\langle \Phi_0^* | \Phi_0 \rangle} \quad (3.5)$$

In the HF approach, the antisymmetry of the electronic wavefunction (eq. 3.6) is guaranteed by constructing the wave function as a Slater determinant (eq. 3.7) – a linear combination of  $n$  orthonormal one-electron atomic orbitals (eq. 3.8) (products of one spatial and one spin orbital):

$$\Phi_k(x_1, \dots, x_i, \dots, x_j, \dots, x_N) = -\Phi_k(x_1, \dots, x_j, \dots, x_i, \dots, x_N) \quad (3.6)$$

$$\Phi_k = \frac{1}{\sqrt{n!}} \begin{vmatrix} \psi_1(x_1) & \psi_1(x_2) & \cdots & \psi_1(x_n) \\ \psi_2(x_1) & \psi_2(x_2) & \cdots & \psi_2(x_n) \\ \vdots & \vdots & \ddots & \vdots \\ \psi_n(x_1) & \psi_n(x_2) & \cdots & \psi_n(x_n) \end{vmatrix} \quad (3.7)$$

$$\psi_i(x_j) = \psi_i(\mathbf{r}_j, \sigma_j) = \varphi(\mathbf{r}_j) \chi(\sigma_j) \quad (3.8)$$

With suitable transformations of both the operator,  $\hat{h}_e \rightarrow \hat{\mathcal{F}}$  and wavefunction  $\psi_i \rightarrow \psi'_i$ , the variational derivation gives the single electron HF equations in (3.9), cast in the form of the Schrödinger equation. Operating on the atomic orbitals  $\psi'_i$  with the Fock operator  $\hat{\mathcal{F}}$ , the energy eigenvalues  $\varepsilon_i$  are obtained, which are related to the total HF energy according to (eq. 3.10). Overall, three terms contribute to the total electronic HF energy; one term from the one-electron operators,  $\hat{T}_e$  and  $\hat{V}_{Ne}$ , and two terms from the two-electron operator,  $\hat{V}_{ee}$  (eq. 3.11).

$$\hat{\mathcal{F}}\psi'_i = \varepsilon_i \psi'_i \quad (3.9)$$

$$E^{HF} = \sum_{i=1}^n \varepsilon_i - \frac{1}{2} \sum_{i=1}^n \sum_{j=1}^n (J_{ij} - K_{ij}) \quad (3.10)$$

$$\varepsilon_i = E_{ii} + \sum_{i=1}^n \sum_{j=1}^n (J_{ij} - K_{ij}) \quad (3.11)$$

$$E_{ii} = \langle \psi'_i | \hat{T}_{e,i} + \hat{V}_{Ne} | \psi'_i \rangle; \quad J_{ij} = \langle \psi'_i \psi'_j | \hat{V}_{ee} | \psi'_i \psi'_j \rangle; \quad K_{ij} = \langle \psi'_i \psi'_j | \hat{V}_{ee} | \psi'_j \psi'_i \rangle$$

Accordingly,  $E_{ii}$  is the sum of the kinetic energy of a single electron and a potential energy contribution from the interaction of the electron with the static nuclei, and  $J_{ij}$  and  $K_{ij}$  are the coulomb repulsion and exchange repulsion energies, respectively.

Practically, most HF computations are performed by solving a modified set of equations known as the Roothaan-Hall equations that were developed in the 1950s and have an appropriate form for implementation in computer software. In these equations the atomic orbitals of (eq. 3.7) are constructed from mathematical functions known as *basis sets*.

Beyond the HF-theory, more elaborate theories are built on the basic HF-theory, by accounting for electron correlations in a more accurate way. Theories have been developed where either the HF Hamiltonian is modified or where more than one determinant is used to represent the total wavefunction. The former approach includes the *perturbation theory* developed by Møller and Plesset (MP).<sup>148</sup> In this approach, a second term is added to the HF Hamiltonian (eq. 3.12), which leads to an unperturbed energy (the first term of eq. 3.10), and a series of energy correction terms. The order of the approach, MP(X), depends on how many energy correction terms are evaluated and added to the zeroth order term (eq. 3.13).

$$\hat{h}_e^{MP2} = \hat{h}_e^{HF} + \Delta\hat{h}_e \quad (3.12)$$

$$= \sum_{i=1}^n \hat{\mathcal{F}}_i + \left[ \frac{1}{2} \sum_{i \neq j}^n \frac{1}{|\mathbf{r}_i - \mathbf{r}_j|} - \sum_{i=1}^n \sum_{j=1}^n (\hat{J}_{ij} - \hat{K}_{ij}) \right]$$

$$E^{MP(X)} = E^{(0)} + E^{(1)} + \dots + E^{(X)} \quad (3.13)$$

In this work the second order approach (MP2) has been used. For an estimate of the quality of HF and MP2 results, the HF approach offers very good predictions of minimum-energy structures and thus may be used to screen for equilibrium structures. However, with regard to the structural parameters, the HF approach tends to underestimate experimentally determined bond distances. With MP2 improved predictions of energy differences between different equilibrium structures are possible and improved calculated bond distances are obtained.<sup>149</sup>

### **Density functional methods**

Density functional theory (DFT) is an alternative approach with a practical origin in the work of Hohenberg, Kohn, and Sham in the 1960s.<sup>150-151</sup> The result of the basic theorem of DFT is that for every unique electron density of a system (eq. 3.14), there exists a unique energy.<sup>150</sup> Therefore, the system energy is a functional of the electron density,  $E[n(\mathbf{r})]$ , and in particular, the ground-state energy is a function of the ground-state electron density (eq. 3.15). The practical form of the general energy density

functional was introduced by Kohn and Sham (KS),<sup>151</sup> who proposed to separate the known and unknown energy contributions to the overall energy, and collect the unknown contributions in a single exchange-correlation term,  $E_{xc}[n]$  (eq. 3.16).

$$n(\mathbf{r}) = \sum_{i=1}^n |\psi_i|^2 \quad (3.14)$$

$$E_0^{DFT} = \langle \psi_i^* | \hat{h}_e | \psi_i \rangle = - \int \frac{Z_i}{|\mathbf{R}_i - \mathbf{r}_i|} n_0(\mathbf{r}) d\mathbf{r} + F[n_0(\mathbf{r})] \quad (3.15)$$

$$E^{KS}[n] = \int V_{ext} n(\mathbf{r}) d\mathbf{r} + T_0[n] + E_H[n] + E_{xc}[n] \quad (3.16)$$

With this division, the remaining terms represent energies of a non-interacting system and are therefore exactly known; the interaction of the electron density with the frozen nuclei, the kinetic energy of non-interacting electrons,  $T_0$ , and the classic electrostatic electron-electron (Hartree) interactions,  $E_H$ . Similar to the wavefunction methods, the variational minimization of the KS energy expression (eq. 3.16) leads to a Schrödinger-type equation (eq. 3.17) that can be iteratively solved until a self-consistent solution is found. The corresponding total KS ground-state energy is obtained from (eq. 3.18).

$$\left[ -\frac{1}{2} \nabla_i^2 + \hat{v}_{eff} \right] \psi_i(\mathbf{r}) = \varepsilon_i \psi_i(\mathbf{r}) \quad (3.17)$$

$$\hat{V}_{eff} = \hat{V}_H + \hat{V}_{ext} + \hat{V}_{xc}$$

$$\hat{V}_H(\mathbf{r}) = \left[ \int \frac{n(\mathbf{r}')}{|\mathbf{r} - \mathbf{r}'|} d\mathbf{r}' \right]; \quad \hat{V}_{ext}(\mathbf{r}) = \left[ - \sum_{i=1}^n \frac{Z_i}{|\mathbf{R}_i - \mathbf{r}|} \right]; \quad \hat{V}_{xc}(\mathbf{r}) = \left[ \frac{\delta E_{xc}}{\delta n(\mathbf{r})} \right]$$

$$E_0^{KS} = \sum_{i=1}^n \varepsilon_i - \frac{1}{2} \int \int \frac{n(\mathbf{r})n(\mathbf{r}')}{|\mathbf{r} - \mathbf{r}'|} d\mathbf{r}d\mathbf{r}' + E_{xc}[n] - \int V_{xc}(\mathbf{r})n(\mathbf{r})d\mathbf{r} \quad (3.18)$$

In contrast to the wavefunction approaches, the density functionals contain a mix of exchange and correlation effects – without treating any of them exactly. Therefore, the performance depends strongly on the quality of the approximate exchange-correlation term. Also, unlike the wavefunction methods, no systematic improvements are available among the DFT approaches. However, still different DFT approaches can be sorted, depending on the sophistication of the approximation of the  $E_{xc}$  term. Normally this term is composed of one exchange,  $E_x$ , and one correlation,  $E_c$ , term.

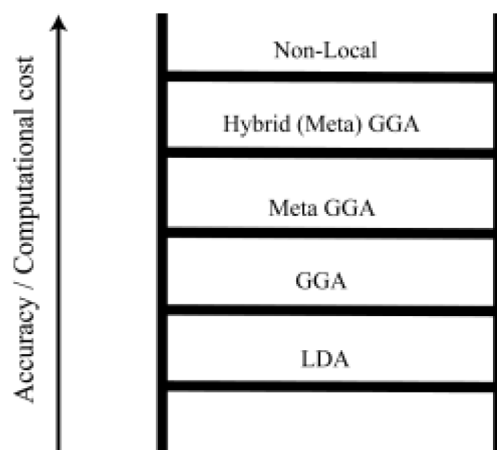


**Figure 8.** “Jacob’s ladder” is a classification of density functionals according to the sophistication of the exchange-correlation approximations. For a more artistic representation of the ladder see ref. [152].

The dependence of either of these terms on the electron density can be direct, as in the local density approximation (LDA), or involve also the gradient of the electron density, as realized with the generalized gradient approximation methods (GGAs). These approximations represent the first two steps of a density functional sophistication ladder<sup>152-153</sup> (Figure 8). On this ladder, the different functionals are arranged between the HF accuracy (below the ladder) and the exact solution (above the ladder). Of the functionals used in this work, the Van Voorhis and Scuseria exchange correlation (VSXC)<sup>154</sup> functional is of the meta-GGA type and the Becke (3-parameter), Lee, Yang, and Parr (B3LYP)<sup>155</sup> functional is of hybrid GGA type. The hybrid functional refers to that a certain percentage of exact exchange from HF-theory is mixed with the exchange-correlation from a GGA approach, which has become the most popular approach for molecular systems.<sup>156</sup>

Compared to the extended HF-theories, the benefits of DFT is the high accuracy obtained at a much lower computational cost. With an increase in the size of the mathematical representation (basis sets) of the orbitals, the increase in computational time (scaling) is smaller for the density functionals, compared to the wavefunction methods. Drawbacks of the DFT technique are mainly the poor ability to account for excited state properties and the appearance of spurious errors, even for ground-state computations. More detailed comparisons of different approaches within and between the two families of electronic structure methods are available in several textbooks and review articles.<sup>145-146,149,156</sup> Recommended are also two short pedagogical introductions to the key concepts of DFT.<sup>152,157</sup>

### **Continuum-solvent models**

The complexity of a quantum mechanical model is limited by the computation time and ultimately the available computational resources, which makes it impossible to model full-scale electrolytes. Fortunately, to a good approximation, realistic electrolyte properties can be predicted from very small model systems, based on a single or a few components. However, there exist also several possibilities to extend the size of a model by introducing an implicit surrounding; the solvent environment of an anion can, for example, be modelled with a continuum solvent approach.<sup>158</sup>

In the polarizable continuum model (PCM),<sup>159</sup> and variants thereof (for example C-PCM),<sup>160-161</sup> a cavity is constructed around the solute, typically by fusing van der Waals<sup>162-163</sup> spheres centred on all (or some) of the solute atoms. The electrostatic solute/solvent interactions are modelled by the interactions of the solute with “apparent” charges forming a discrete or continuous distribution at the cavity surface. Practically, the Hamiltonian of the solute is modified with a solute-solvent interaction potential, known as a solvent reaction potential, that describe the polarizing effect of the charged surface on the solute and vice versa. Thus, a self-consistent solution with respect to the new Hamiltonian requires also a self-consistent solvent reaction field. Apart from the charged cavity surface, other solvent-solute interactions, such as dispersive and repulsive interactions, are taken into account in relation to a set of additional solvent accessible (SAS) and solvent excluded surfaces (SES).

Overall, the result of the continuum approach is the evaluation of a minimum free energy of solvation,  $G_0^{cont}$ , that is composed of several contributions (eq. 3.19). In addition to the aforementioned electrostatic, dispersive and repulsive terms, also a free energy of cavity formation is included.<sup>164</sup>

$$G_0^{cont} = G_{el} + G_{disp} + G_{rep} + G_{cav} \quad (3.19)$$

### **Basis Sets**

For computational convenience the Roothaan-Hall or Kohn-Sham orbitals of HF and DFT theory, respectively, are represented by basis sets; linear combinations of a restricted number of basis functions,  $\phi$  (eq. 3.20).

$$\psi'_p = \sum_{q=1}^Q \sum_{r=1}^R c_{p,q} \phi_r \quad (3.20)$$

The basis functions are commonly (not always) exponential functions known as Cartesian Gaussian-type orbitals (GTOs). The GTOs are not the most suitable choice for an accurate representation of the electron distribution in an atom, but they are convenient from a computational point of view, since an analytical evaluation of all SCF integrals is possible. Their insufficiency is compensated for by forming linear

combinations, contracted GTOs, of several primitive GTOs.<sup>147</sup> These contracted GTOs are constructed to fit the more representative, but computationally hard to handle Slater-type orbitals (STOs). The combination of primitive GTOs and contracted GTOs, used for describing the orbitals of an atom, are known as basis sets, of which there exist several families with different nomenclatures. In this work Pople-type basis sets are used.

Exemplified by the 6-311+G(2df,p) basis set, the existing nomenclature for the Pople basis sets first gives the number of primitive GTOs (6) used to construct one contracted GTO for representing the core electrons of heavy atoms. After the dash the subsequent numbers (-311) indicate the functions used to represent the valence electrons, in terms of one contracted GTO (based on three primitive GTOs) and two primitive GTOs. The plus sign (diffuse functions) and the letters within parenthesis (polarization functions) describe the use of additional GTOs to create more flexible basis sets, especially required for anions, which have more diffuse electron distributions compared to neutral species and cations.

To specify whether additional functions are used only for heavy atoms (all atoms but the hydrogen atom) or for all atoms, one or two plus signs are included for the diffuse functions; a comma makes the same distinction for the polarization functions. The letters of the polarization description indicate the *orbital angular momentum* of the polarization functions, in line with common conventions for atomic orbitals.<sup>146</sup> In the example given above, a diffuse function is added to the heavy atoms along with two d-type and one f-type polarization function. In addition a p-type polarization function is added to the hydrogen atoms.

### ***Computed Molecular Properties***

The approaches outlined above are recipes for calculating the electronic minimum energy for a fixed nuclei configuration. The total energy can be explored as a function of the nuclei positions, to obtain a multidimensional potential energy surface (PES), where each nuclei configuration gives rise to a single point on the surface. A representative example is the partial PES of the FSI anion,<sup>165</sup> as a function of the two dihedral FSNS angles (Figure 9). A special case is to search for a minimum energy structure from a starting structure.

To confirm that an optimized structure corresponds to an energy referred to as a minimum, and not a possible transition state (local energy maximum), the second derivative of the energy with respect to the nuclear coordinates is evaluated. Exploring the curvature close to an energy minimum, the harmonic vibration frequencies for the structure can be predicted. Analytical infrared (IR) intensities are evaluated simultaneously, in the form of the polarizability – the second derivatives of the energy with respect to an applied electric field.<sup>166</sup> Raman activities, are obtained from the derivative of the polarizability with respect to the nuclear coordinates,<sup>167</sup> this being a third derivative property.

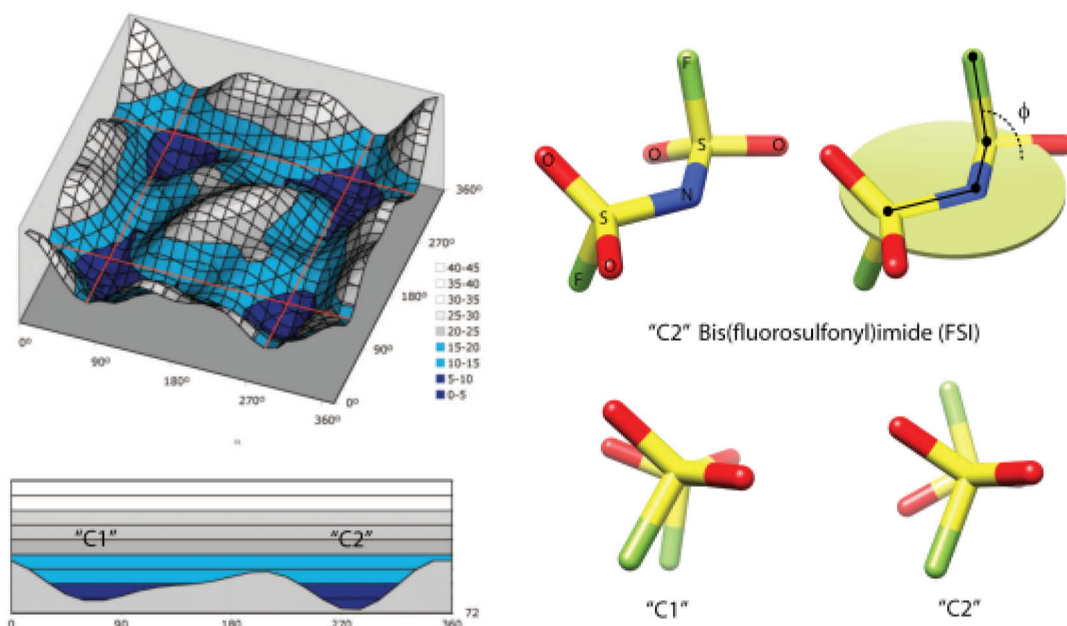


**Figure 9.** Left: Potential energy surface (PES) for FSI, as a function of the two dihedral FSNS angles. Reprinted with permission from [165], Copyright 2008 American Chemical Society. Right: optimized “C1” and “C2” conformers of FSI [B3LYP/6-311+G(d)].

The calculated vibration properties of anions, isolated and associated with  $\text{Li}^+$  and/or solvent molecules, are valuable for analyzing spectroscopic data (see next section). Detailed examples for lithium battery electrolytes; liquids, gels, and especially polymers, are available in reference [168]. There, a number of properties of lithium battery electrolytes that can be addressed by *ab initio* computations are reviewed. The properties most relevant for this work are introduced below.

#### ANION OXIDATION STABILITY

In seminal work by Kita et al.,<sup>169</sup> the oxidation stability of several fluorinated anions was estimated by a semi-empirical computational approach, correlating the energies of the HOMO,  $E_{HOMO}$ , to existing experimental data. The same approach, but based on *ab initio* (HF) computations, was adopted by Ue et al.<sup>170</sup> The basis set dependence was investigated and a second approach was implemented; using DFT (B3LYP), the authors explored the concept of a vertical ionization potential (transition energy)  $\Delta E_v$  – the removal of an electron from the anion, without a change in the nuclear configuration (eq. 3.21; the Franck-Condon principle).<sup>171</sup> The DFT predictions offered the best agreement with experimental results,<sup>170</sup> which was attributed to the account of electron correlation in this approach.

$$\Delta E_v = E_{radical} - E_{anion} \quad (3.21)$$

The  $E_{\text{HOMO}}$  and  $\Delta E_{\text{v}}$  approaches were further tested by Johansson, for a set of twelve structurally diverse anions,<sup>143-144</sup> semi-empirical, HF, and DFT approaches were all used to predict both  $E_{\text{HOMO}}$  and  $\Delta E_{\text{v}}$ . In addition, the effect of solvation was addressed via the vertical free energy transition,  $\Delta G_{\text{v}}$ , from C-PCM calculations. The results, lead to recommend to calculate  $\Delta E_{\text{v}}$  VSXC/6-311+G(2df,p), as an efficient and accurate approach.<sup>143</sup> This is the basic approach adopted in this work.

### *ION PAIR DISSOCIATION ENERGY*

The ion pair dissociation energy,  $E_{\text{d}}$  (eq. 3.22), is a measure of the interaction strength between  $\text{Li}^+$  and one anion. It is a good approximation to the lattice energy of metal salts,<sup>172</sup> and is used to compare different lithium salts; the smaller the energy difference, the more dissociative the salt.

$$E_{\text{d}} = (E_{\text{anion}} + E_{\text{cation}}) - E_{\text{salt}} \quad (3.22)$$

The energies of different lithium ion pair configurations also offer insight to the preferred configuration of interaction. Taking  $\text{LiBF}_4$  as an example, three ion pair configurations (mono, bi, and tridentate) were identified by ab initio calculations over three decades ago.<sup>173</sup> Of these, the bidentate  $\text{LiBF}_4$  configuration was predicted to be the most stable. The  $\text{LiBF}_4$  ion pair has since been revisited many times; at different computational levels,<sup>174</sup> to address the effects of a solvent surrounding – implicit<sup>175</sup> or explicit<sup>176-178</sup> – and frequently to assist the interpretation of spectroscopic data.<sup>174,176-178</sup> Different approaches to lithium ion dissociation have been compared for several common lithium salts, including  $\text{LiBF}_4$ .<sup>179</sup> The results demonstrate that the most stable ion pair configuration, and relative lithium salt dissociation energies, can change between different approaches.

Dissociation energies of a large selection of lithium salts, in vacuum or implicitly solvated, have been compared and correlated with calculated anion volumes.<sup>180</sup> The anion volume is important for the anion mobility and the overall transport properties of the electrolyte, and can be conveniently estimated computationally.<sup>180-181</sup> However, for the ease of ion pair dissociation, the anion volume has suggested to be of secondary importance,<sup>180</sup> and it has been given less attention in this work.

## **3.2 Raman Spectroscopy**

The quantized energy levels of atoms and molecules are the source of the typical discrete responses observed when electromagnetic radiation interacts with matter. Of the many spectroscopic tools developed, Raman spectroscopy has been used in this work, as a probe of molecular vibrations.<sup>182</sup> The experimental origin of Raman spectroscopy is attributed to the Indian scientists Raman and Krishnan,<sup>183</sup> who confirmed the theoretical predictions of Smekal. Today, Raman spectroscopy is a

versatile technique – easy to use – due to development of lasers and advances made in the experimental instrumentation. The development of spectrometers relying on interferometers, Fourier transform (FT) techniques, has made it possible to analyze scattered radiation of multiple wavelengths simultaneously (Fellgett advantage).<sup>171</sup> Also, more radiation can be passed through the spectrometer and collected by improved detectors, without a sacrifice in signal-to-noise ratio (Jaquinot advantage).

It is straight-forward to record a Raman spectrum from a molecular sample, since for most purposes, a small volume of sample in a sealed glass vial is an adequate prerequisite. Furthermore, the energy of the radiation can exceed the energy differences between two discrete energy levels of the molecule. However, the molecules have to be anisotropically polarizable; in an electric field, the electron distribution should be unequally disturbed in different directions. A popular introduction to the Raman scattering phenomenon is based on a classical description of the interacting system (see reference [<sup>182</sup>] for details). Accordingly, a dipole moment,  $\mathbf{p}$ , is induced in a molecule, due to the electric field,  $\mathbf{E}$ , of the incident radiation (eq. 3.23). Accounting only for the linear dependence of  $\mathbf{p}$  on  $\mathbf{E}$ , the property relating the two is the molecule polarizability,  $\boldsymbol{\alpha}$  (a 3x3 tensor).

$$\mathbf{p} = \boldsymbol{\alpha} \cdot \mathbf{E} \quad (3.23)$$

The collective motions of all atoms in the molecule can be represented by vibrational normal coordinates (internal nuclear coordinates)  $Q_i$ . If  $\boldsymbol{\alpha}$  is expanded in terms of  $Q_i$ , around the equilibrium structure, a description is obtained for the change in polarizability during each molecular vibration. If the expansion is a Taylor series (truncated at the second term) and explicit expressions for  $\mathbf{E}$  and harmonic  $Q_i$  (eq. 3.24) are introduced, the result is a three-term expression for the oscillation of  $\mathbf{p}$  (eq. 3.25).

$$\mathbf{E} = E_0 \cos(\omega_L t) \quad ; \quad Q_i = Q_{i,0} \cos(\omega_i t) \quad (3.24)$$

$$\mathbf{p} = \mathbf{p}_R + \mathbf{p}_S + \mathbf{p}_A \quad (3.25)$$

$$\mathbf{p}_R = \alpha_{ij,0} E_0 \cos(\omega_L t)$$

$$\mathbf{p}_S = \left( \frac{\partial \alpha_{ij}}{\partial Q_i} \right)_0 Q_{i,0} E_0 \cos[(\omega_L - \omega_i)t] \quad ; \quad \mathbf{p}_A = \left( \frac{\partial \alpha_{ij}}{\partial Q_i} \right)_0 Q_{i,0} E_0 \cos[(\omega_L + \omega_i)t]$$

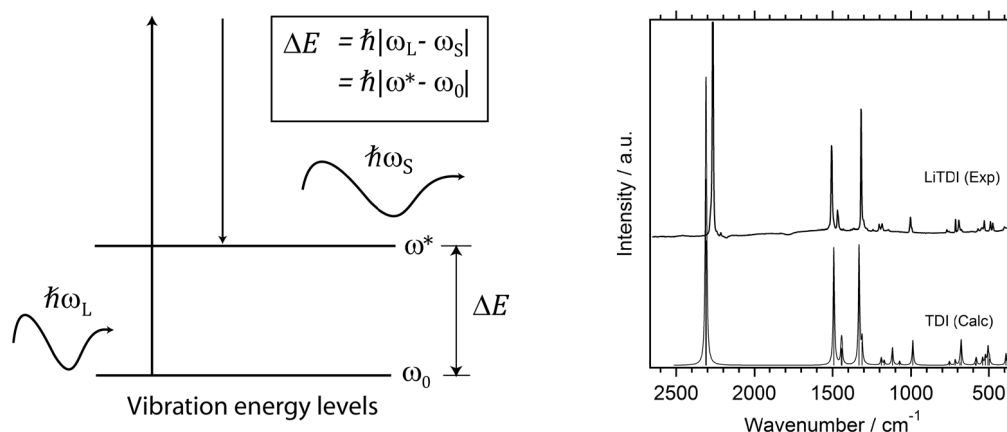


**Figure 10.** Energy diagram illustrating the principle of Stokes Raman scattering (left). Experimental and calculated examples of Stokes Raman spectra (right).

The first component,  $\mathbf{p}_R$ , is of the same angular frequency ( $\omega_L$ ) as the electric field and is responsible for Rayleigh scattering. The second and third components,  $\mathbf{p}_S$  and  $\mathbf{p}_A$ , have either lower or higher angular frequencies compared to the electric field, and are responsible for the Raman scattered radiation. More specifically, the low and high frequency components lead to Stokes and anti-Stokes scattering, respectively. The frequency change is due to a transfer of energy from the electric field to the molecule (Stokes) or vice-versa (anti-Stokes).

At ambient temperatures, most molecules are in the vibration ground state, which makes Stokes scattering more probable, therefore more intense. The principle of Stokes scattering and examples of experimental and calculated Stokes Raman spectra are presented in Figure 10. The interaction between the sample and the radiation is instantaneous, during which the energy of the interacting system exceeds that of the molecule alone. The energy transferred between the photon and the molecule,  $\Delta E = E(\omega^*) - E(\omega_0)$ , corresponds to that between the initial,  $\omega_0$ , and final,  $\omega^*$ , vibrational state of the molecule. In a Raman spectrum, the scattered radiation gives rise to discrete bands with observable widths, to which there are several (broadening) contributions. Band shapes, intensity and polarization of scattered light also carry information. However, in this work, the main analyses are based on observed changes in band positions. The band positions are given in units of wavenumber ( $\tilde{\nu} / \text{cm}^{-1}$ ), in which most molecular vibrations span the interval  $0 < \tilde{\nu} < 4000 \text{ cm}^{-1}$ .

## 4 SUMMARY OF RESULTS

### 4.1 Ion pair dissociation and anion stability

A dissociation-stability plot is a convenient format to analyze new anions (Figure 11). The ion pair dissociation energy decreases from right to left and the anion oxidation stability increases from down and up. Consequently, the most promising lithium salts are located in the top left corner.

The results from paper I-III are summarized in Figure 11. Each paper is a study of structurally related anions representative of a distinct class or family of lithium salts. The distinction made here refers to the approximate geometry of the anions; spherical (paper I), planar (paper II), or linear (paper III) (Figure 11a). A clear separation of the different families of salts is observed and within each family both ion pair dissociation energies and anion stabilities increase when classic fluoro anions are redressed as cyano alternatives (Figure 11b). The results suggest that there is room for improvements within each family of salt, considering the archetypical (LiPF<sub>6</sub>, LiBF<sub>4</sub>, LiTFSI, and LiFSI) lithium salts or the less well-known, but available LiTADC (Figure 11c). New lithium salts that have already emerged, are predicted to offer an improvement of one (LiTDI) or both properties (LiB(CN)<sub>4</sub> = LiBison). Two main questions to discuss in relation to these results are; 1) if the results are consistent between different approaches, and most importantly 2) how (or if) the results are of relevance for real electrolyte properties.

The first question is addressed by comparing the DFT results (Figure 11a, b, and c) with corresponding HF results (Figure 11d, e, and f). The HF results are more spread out and the absolute scales are different, however, most important are the qualitative differences obtained for the cyano and fluoro based spherical anions. The HF results suggest a lower intrinsic stability of the As(CN)<sub>6</sub><sup>-</sup>, P(CN)<sub>6</sub><sup>-</sup>, and Bison anions compared to AsF<sub>6</sub><sup>-</sup>, PF<sub>6</sub><sup>-</sup>, and BF<sub>4</sub><sup>-</sup>. The single strongest effect is the substantial drop (~2 eV) observed when one of the fluoro atoms of BF<sub>4</sub><sup>-</sup> is replaced by a cyano substituent, BF<sub>3</sub>(CN)<sup>-</sup>. Perfluorination of BF<sub>4</sub><sup>-</sup> into BF<sub>3</sub>(CF)<sub>3</sub><sup>-</sup> has been experimentally observed to destabilize BF<sub>3</sub>(CF)<sub>3</sub><sup>-</sup> 1 V with respect to BF<sub>4</sub><sup>-</sup>, a result corroborated by HF calculations of the corresponding  $E_{HOMO}$ . The same qualitative result is predicted also with the VSXC approach (5.2 → 4.7 V vs. Li<sup>+</sup>/Li<sup>0</sup>). From the higher overall accuracy of the VSXC method,<sup>143</sup> the results for the spherical anions using this method is expected to be the more reliable.

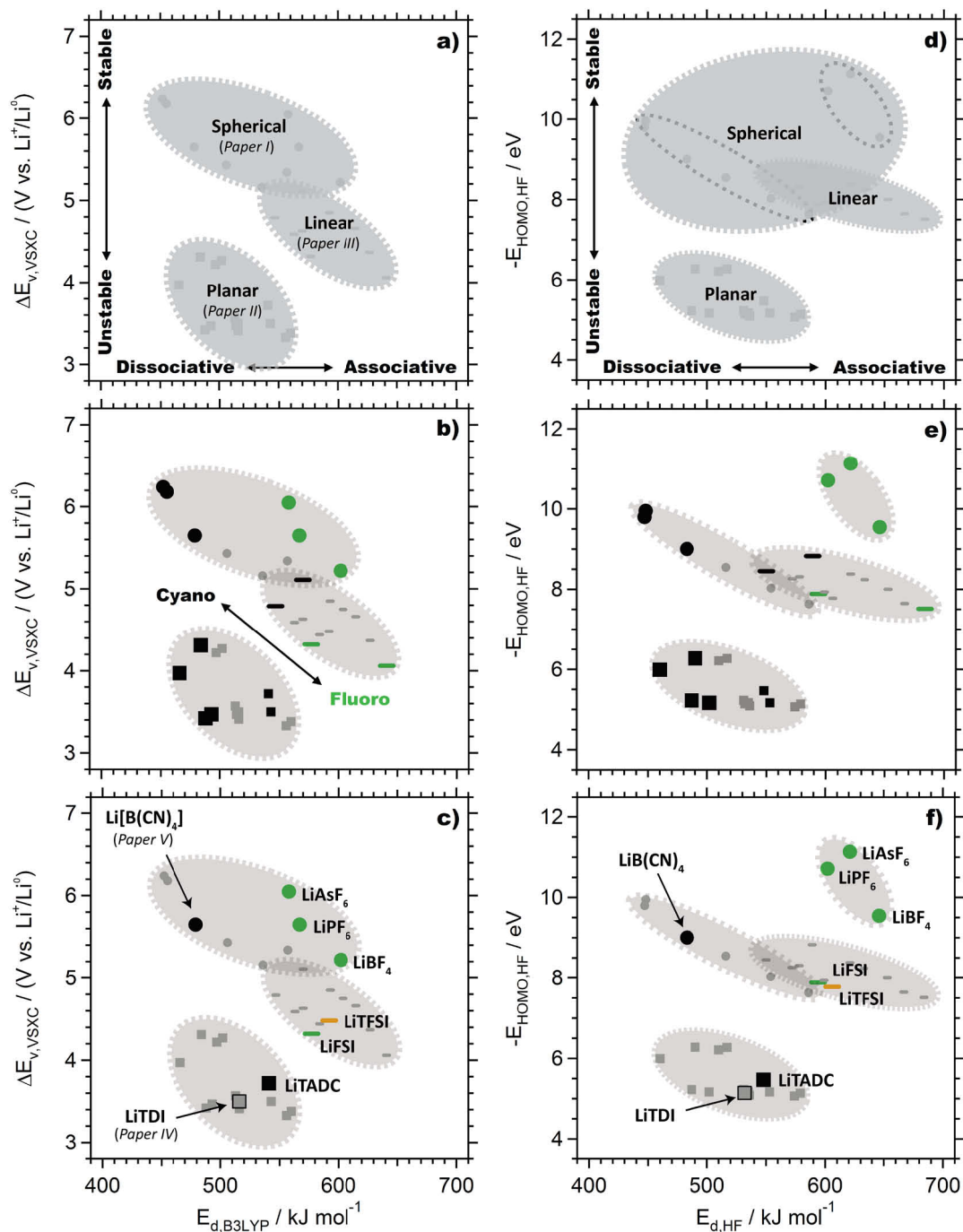


**Figure 11.** Dissociation-stability plots for the anions studied in paper I, II, and III. The results in the left column are from DFT calculations and in the right column are HF results. LiX dissociation energies,  $E_d$ , decrease from right to left and anion oxidation stability,  $\Delta E_v$ , increase from down and up.

The possibility to corroborate the results of Figure 11 is difficult, since neither property has a direct experimental analogue. The intrinsic anion oxidation stability is correlated to experimental oxidation potentials,  $E_{ox}$ , measured by linear sweep voltammetry (LSV). Different computational approaches have been validated with respect to LSV results.<sup>143-144</sup> However, the calculated intrinsic anion stabilities avoid the deficiencies

of experimental setups and the specific environment. The ambiguities involved in determining experimental oxidation potentials by LSV, the implications for comparing results from different sources, and the relevance of the results for the stability in a complete cell, have been concisely summarized in the final paragraphs of ref. [170]. These issues have also been addressed by Xu,<sup>48</sup> stressing the differences obtained with respect to either “inert” (Au, Pt, glassy carbons) electrodes or “active” composite cathode surfaces.

Nevertheless, the idea of an intrinsic anion oxidation potential is appealing and can be imagined as a theoretical upper oxidation limit – *possibly* realized in combination with suitable solvents and electrode materials. Thus, the anion stability results of Figure 11 should foremost stimulate an unconventional inside-out approach to lithium battery design, a reversal of the common procedure of applying new lithium salts to environments optimized for LiPF<sub>6</sub>. A discussion of the ion pair dissociation results is made in connection with the experimental results on the electrolytes of paper I, IV, and V.

## 4.2 Ion interactions in LiTDI and XBison electrolytes

Lithium salt dissociation in electrolytes depends on the solvent. Electronic structure calculations on simple ion pair models are used to compare and rank Li<sup>+</sup> – anion interactions. However, no direct information is provided on the salt solubility, which is driven by changes in the free energy (enthalpy + entropy). Instead, a straight-forward connection with experiments is through the relative stabilities of predicted ion-pair configurations.

In paper IV, Raman spectroscopy and several tentative ion-ion and ion-solvent models were used to probe the local environment in LiTDI based electrolytes, as a function of solvent and salt concentration. The spectroscopic signatures of the predicted minimum energy ion pair configuration (paper II) were found to be in qualitative agreement with the experimental signatures (Figure 12a), suggesting that Li<sup>+</sup> preferentially coordinates to the imidazolide nitrogen. From refined models, taking into account implicit or explicit (Figure 12b) solvent effects, the experimental results were reproduced with high accuracy. Also, where detected, the signatures of ion-ion coordination were found to be similar, irrespective of the solvent. This demonstrated the possibility of, if needed, using poor electrolyte solvents to ease the identification of the preferential anion coordination sites for Li<sup>+</sup>, prior to a quantitative analysis of ion associates in more realistic battery electrolytes. However, overlapping signatures originating from several associates do introduce some ambiguity in deciphering the specific Li<sub>x</sub>TDI<sub>y</sub> associates present in the electrolyte.

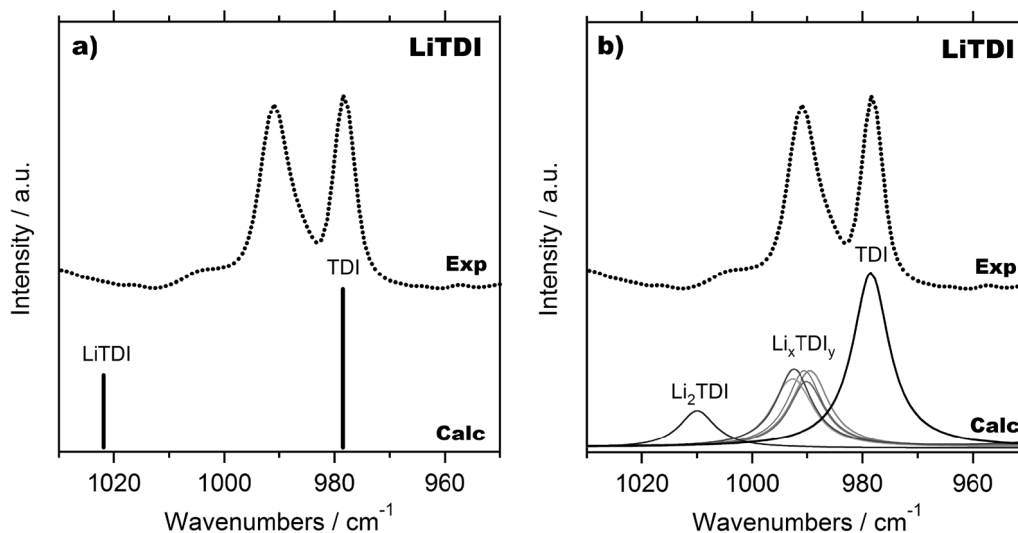


**Figure 12.** a) experimental Raman spectrum of 1M LiTDI in acetonitrile and calculated signatures for the most stable ion pair, b) same experimental spectrum, compared with calculated Raman bands for several explicit  $\text{Li}_x\text{TDI}_y$  associates. All calculated spectra have been shifted horizontally (uniformly in each window) to ease the comparison of experimental and calculated results. A Lorentzian broadening has been applied to the calculated spectra of b).

The results of studies on Bison ILs (paper I and V) and XBison electrolytes ( $X = \text{Li}, \text{Na}, \text{K}$ ; paper V) further illustrate the power of a combined computational and experimental approach. In particular, superb qualities of neat ILs, such as high ionic conductivity and low viscosity, are no guarantees for successful implementation as solvents for electrolytes. The solubility of LiBison in Bison based ILs is poor, which is contrasted by the facile dissolution of  $\text{LiBF}_4$  in  $\text{BF}_4^-$  based ILs. In vacuum, the predicted dissociations of these salts represent opposite extremes (Figure 11) – LiBison being the most dissociative.

The suggested rationale for the poor LiBison solubility is a stabilization of the monodentate  $\text{Li}^+$  coordination in a dielectric environment, in combination with a high symmetry anion. These results are based on dissociation energies for implicitly solvated ion pairs and extended  $\text{Li}[\text{Anion}]_4^{3-}$  associates. The latter results suggest that the  $\text{Li}[\text{Bison}]_4^{3-}$  associates are more stable compared to the  $\text{BF}_4^-$  based analogues (Figure 13a). These predictions are supported by a Raman spectroscopic analysis (Figure 13b). No similar changes in coordination preferences have been predicted for the linear or planar heterocyclic anions. Thus, Bison based electrolytes are realized only in strong  $\text{Li}^+$  coordinating oligomer/polymer environments. A recently introduced concept of oligoether doped ILs,<sup>88</sup> is found not to be a viable approach for LiBison (unpublished results). Demonstrated in paper V is also the reversible intercalation of  $\text{Li}^+$  in  $\text{LiFePO}_4$ , with excellent capacity retention, using a  $\text{Li/LiBison}:\text{PEGDME}/\text{LiFePO}_4$  cell.

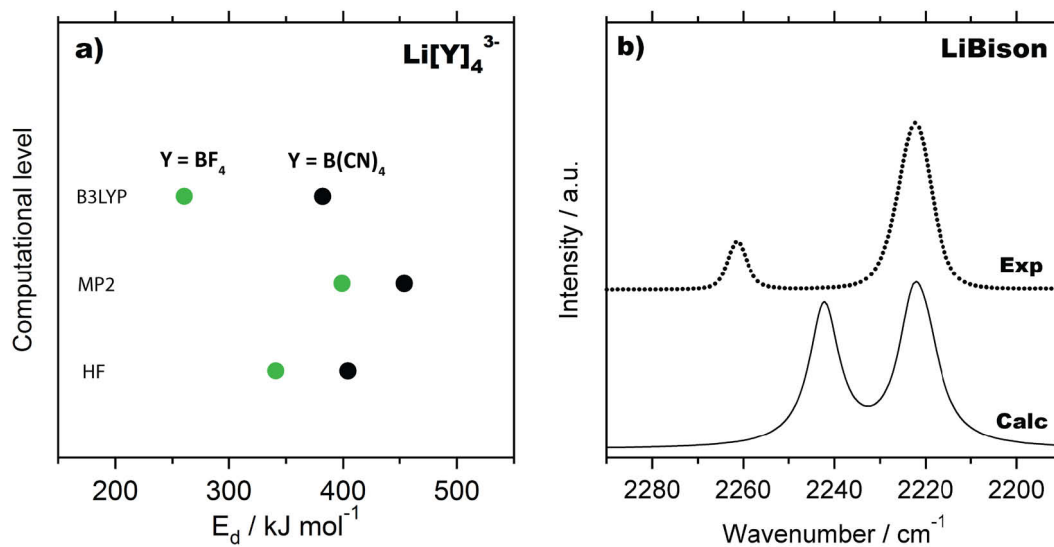


**Figure 13.** a) dissociation energies of the explicit four-coordinated lithium ion associates,  $\text{Li}[\text{BF}_4]_4^{3-}$  and  $\text{Li}[\text{B}(\text{CN})_4]_4^{3-}$ . The order of energies is reversed compared to the ion pair energies of Figure 11, b) Raman spectra of the  $\nu(\text{CN})$  mode of 1M LiBison in  $\text{C}_2\text{mimBison}$  and calculated Raman bands of the  $\text{Li}[\text{B}(\text{CN})_4]_4^{3-}$  model.



## 5 CONCLUSIONS AND OUTLOOK

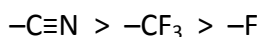
- ✓ Calculated intrinsic anion oxidation stabilities ( $\Delta E_v$ ) and ion pair dissociation energies ( $E_d$ ) offer an opportunity to rank new anions and lithium salts.

How do these results change if an explicit polarizing solvent, lithium ion, or surface is taken into account? The former have been addressed in part, but further studies should be able to reveal possible qualitative and quantitative differences.

- ✓  $\Delta E_v$  and  $E_d$  are related to the anion structure, the number of substituents – their type and position. Classes of anions with different geometric characteristics; planar, linear, or spherical, map out distinct regions in  $E_d$ - $\Delta E_v$  space.

Do the large differences between anion classes make a comparison valid over anion “families”? More anion classes remain to be included.

- ✓ Changes in  $\Delta E_v$  and  $E_d$  are systematic within each class of anions and both properties show the same functional group dependence:



$\Delta E_v$  and  $E_d$  are two important properties, out of many. The volume and thermal stability of anions are examples of other properties that need to be explored further.

- ✓ Ion pair configurations predicted in vacuum are good first approximations to the local structures in electrolytes. Implicit and explicit solvent effects modify the interaction geometry and, as singular examples, may change the relative stability of alternative configurations.

Computational studies of explicit solute and solvent combinations should address the detailed properties of specific electrolytes.

- ✓ A combined computational and Raman spectroscopic approach is powerful for probing the local electrolyte environment. Detailed comparisons are possible when solvent effects are included in the computational model.

Using spectroscopy, quantitative analysis of ion association in realistic electrolyte should follow the qualitative results of this work.

Overall, *synthesis* efforts should target the lithium salts of each class predicted to be the most promising – the cyano rich compounds. The synthesis of for example LiCSI, have been reported in the patent literature, but its properties need to be addressed more in the scientific community. The possible synthesis routes of many other salts remain to be discovered. *Electrochemical characterization* is crucial to investigate the compatibility of new lithium salts towards the electrolyte and cell components, and to properly address the stability limits. The properties of hybrid anions, contrasted with their anion origins, will be important for an improved understanding of interfacial properties and possible kinetic cell operation. For a coherent picture of the relationship of computational and experimental results, more studies are needed. This is evident from the experimental work on LiTDI and LiBison, with very different solubilities, but similar dissociation in the main computational approach.

To connect to the introduction of this thesis, new batteries for energy applications should be high performing, cost effective, safe, and environmentally benign. Lithium based cells are high performing already today and have an attractive future with respect to the remaining properties. There is an ongoing development of new materials for more sustainable battery technologies – lithium based and others – which include the potentially low-cost lithium-air and lithium-organic cells.<sup>7</sup> New lithium salts will contribute to this development as well. Thus, the *cost, environmental benignity, and toxicity* of the lithium salts presented here, and possible decomposition products, must also be addressed.

## R REFERENCES

- 1 U.S. Department of Energy, [www.energy.gov](http://www.energy.gov)
- 2 Coors, W. G. *Ceramatec* (Santa Clara, CA, USA, 2011).
- 3 Stepien, T. *Primus Power- smart grid storage* (Santa Clara, CA, USA, 2011).
- 4 Park, C.-W. *et al.* Discharge properties of all-solid sodium-sulfur battery using poly (ethylene oxide) electrolyte. *J. Power Sources* **165**, 450-454 (2007).
- 5 Chamberlain, J. *Argonne National Laboratory* (Santa Clara, CA, USA, 2011).
- 6 Chu, S. *Is the Energy Race our new "Sputnik" moment?*, [www.energy.gov](http://www.energy.gov) (29 Nov 2010).
- 7 Armand, M. & Tarascon, J. M. Building better batteries. *Nature* **451**, 652-657 (2008).
- 8 Bard, A. J. & Faulkner, L. R. *Electrochemical Methods - Fundamentals and Applications*. 2nd edn, (Wiley, 2001).
- 9 Winter, M. & Brodd, R. J. What Are Batteries, Fuel Cells, and Supercapacitors? *Chem. Rev.* **104**, 4245-4270 (2004).
- 10 Linden, D. & Reddy, T. R. *Handbook of batteries*. 3rd edn, (McGraw-Hill, 2002).
- 11 Kraysberg, A. & Ein-Eli, Y. Review on Li-air batteries--Opportunities, limitations and perspective. *J. Power Sources* **196**, 886-893 (2011).
- 12 Vincent, C. A. & Scrosati, B. *Modern batteries: an introduction to electrochemical power sources*. 2nd edn, (Butterworth-Heinemann, 1997).
- 13 Tarascon, J. M. & Armand, M. Issues and challenges facing rechargeable lithium batteries. *Nature* **414**, 359-367 (2001).
- 14 Ohzuku, T., Ueda, A. & Nagayama, M. Electrochemistry and Structural Chemistry of LiNiO<sub>2</sub>(R3m) for 4 Volt Secondary Lithium Cells. *J. Electrochem. Soc.* **140**, 1862-1870 (1993).
- 15 Goodenough, J. B. & Kim, Y. Challenges for Rechargeable Li Batteries. *Chem. Mat.* **22**, 587-603 (2010).
- 16 Peled, E. The Electrochemical Behavior of Alkali and Alkaline Earth Metals in Nonaqueous Battery Systems---The Solid Electrolyte Interphase Model. *J. Electrochem. Soc.* **126**, 2047-2051 (1979).
- 17 Verma, P., Maire, P. & Novák, P. A review of the features and analyses of the solid electrolyte interphase in Li-ion batteries. *Electrochim. Acta* **55**, 6332-6341 (2010).
- 18 Winter, M. The Solid Electrolyte Interphase – The Most Important and the Least Understood Solid Electrolyte in Rechargeable Li Batteries. *Zeitschrift für Physikalische Chemie* **223**, 1395-1406 (2009).
- 19 Dominey, L. A. in *Nonaqueous electrochemistry* (ed D. Aurbach) p. 437 (Marcel Dekker, Inc., New York, 1999).
- 20 Aurbach, D., Gofer, Y. & Langzam, J. The Correlation Between Surface Chemistry, Surface Morphology, and Cycling Efficiency of Lithium Electrodes in a Few Polar Aprotic Systems. *J. Electrochem. Soc.* **136**, 3198-3205 (1989).
- 21 Abraham, K. M., Foos, J. S. & Goldman, J. L. Long Cycle-Life Secondary Lithium Cells Utilizing Tetrahydrofuran. *J. Electrochem. Soc.* **131**, 2197-2199 (1984).
- 22 Murphy, D. W., Di Salvo, F. J., Carides, J. N. & Waszczak, J. V. Topochemical reactions of rutile related structures with lithium. *Materials Research Bulletin* **13**, 1395-1402 (1978).
- 23 Lazzari, M. & Scrosati, B. A Cyclable Lithium Organic Electrolyte Cell Based on Two Intercalation Electrodes. *J. Electrochem. Soc.* **127**, 773-774 (1980).
- 24 Mohri, M. *et al.* Rechargeable lithium battery based on pyrolytic carbon as a negative electrode. *J. Power Sources* **26**, 545-551 (1989).
- 25 Naguara, T. & Tozawa, K. Lithium ion rechargeable battery. *Progress in batteries and solar cells* **9**, 209-217 (1990).
- 26 Nishi, Y., Azuma, H. & Omaru, A. Non aqueous electrolyte cell. U.S. patent (1990).
- 27 Fong, R., von Sacken, U. & Dahn, J. R. Studies of Lithium Intercalation into Carbons Using Nonaqueous Electrochemical Cells. *J. Electrochem. Soc.* **137**, 2009-2013 (1990).
- 28 Rao, B. M. L., Francis, R. W. & Christopher, H. A. Lithium-Aluminum Electrode. *J. Electrochem. Soc.* **124**, 1490-1492 (1977).

- 29 Zhang, W.-J. A review of the electrochemical performance of alloy anodes for lithium-ion batteries. *J. Power Sources* **196**, 13-24 (2011).
- 30 Larcher, D. *et al.* Recent findings and prospects in the field of pure metals as negative electrodes for Li-ion batteries. *Journal of Materials Chemistry* **17**, 3759-3772 (2007).
- 31 Hassoun, J., Lee, K.-S., Sun, Y.-K. & Scrosati, B. An Advanced Lithium Ion Battery Based on High Performance Electrode Materials. *J. Am. Chem. Soc.* **133**, 3139-3143 (2011).
- 32 Ferg, E., Gummow, R. J., de Kock, A. & Thackeray, M. M. Spinel Anodes for Lithium-Ion Batteries. *J. Electrochem. Soc.* **141**, L147-L150 (1994).
- 33 Scrosati, B. & Garche, J. Lithium batteries: Status, prospects and future. *J. Power Sources* **195**, 2419-2430 (2010).
- 34 Zaghbi, K. *et al.* Safe and fast-charging Li-ion battery with long shelf life for power applications. *J. Power Sources* **196**, 3949-3954 (2011).
- 35 Edström, K., Gustafsson, T. & Thomas, J. O. The cathode-electrolyte interface in the Li-ion battery. *Electrochim. Acta* **50**, 397-403 (2004).
- 36 Maleki, H., Deng, G., Anani, A. & Howard, J. Thermal Stability Studies of Li-Ion Cells and Components. *J. Electrochem. Soc.* **146**, 3224-3229 (1999).
- 37 Mizushima, K., Jones, P. C., Wiseman, P. J. & Goodenough, J. B.  $\text{Li}_x\text{CoO}_2$  ( $0 < x < 1$ ): A new cathode material for batteries of high energy density. *Materials Research Bulletin* **15**, 783-789 (1980).
- 38 Thackeray, M. M., David, W. I. F., Bruce, P. G. & Goodenough, J. B. Lithium insertion into manganese spinels. *Materials Research Bulletin* **18**, 461-472 (1983).
- 39 Padhi, A. K., Nanjundaswamy, K. S. & Goodenough, J. B. Phospho-olivines as Positive-Electrode Materials for Rechargeable Lithium Batteries. *J. Electrochem. Soc.* **144**, 1188-1194 (1997).
- 40 Ellis, B. L., Lee, K. T. & Nazar, L. F. Positive Electrode Materials for Li-Ion and Li-Batteries†. *Chem. Mat.* **22**, 691-714 (2010).
- 41 Fergus, J. W. Recent developments in cathode materials for lithium ion batteries. *J. Power Sources* **195**, 939-954 (2010).
- 42 Wang, H., Jang, Y.-I., Huang, B., Sadoway, D. R. & Chiang, Y.-M. TEM Study of Electrochemical Cycling-Induced Damage and Disorder in  $\text{LiCoO}_2$  Cathodes for Rechargeable Lithium Batteries. *J. Electrochem. Soc.* **146**, 473-480 (1999).
- 43 Amatucci, G. G., Tarascon, J. M. & Klein, L. C. Cobalt dissolution in  $\text{LiCoO}_2$ -based non-aqueous rechargeable batteries. *Solid State Ion.* **83**, 167-173 (1996).
- 44 Chen, Z., Lu, Z. & Dahn, J. R. Staging Phase Transitions in  $\text{Li}_x\text{CoO}_2$ . *J. Electrochem. Soc.* **149**, A1604-A1609 (2002).
- 45 Xia, Y. *et al.* Improved cycling performance of oxygen-stoichiometric spinel  $\text{Li}_{1+x}\text{Al}_y\text{Mn}_{2-x-y}\text{O}_4$  at elevated temperature. *Electrochim. Acta* **52**, 4708-4714 (2007).
- 46 Imazaki, M., Ariyoshi, K. & Ohzuku, T. An Approach to 12 V "Lead-Free" Batteries: Tolerance toward Overcharge of 2.5 V Battery Consisting of LTO and LAMO. *J. Electrochem. Soc.* **156**, A780-A786 (2009).
- 47 Zhang, W.-J. Structure and performance of  $\text{LiFePO}_4$  cathode materials: A review. *J. Power Sources* **196**, 2962-2970 (2011).
- 48 Xu, K. Nonaqueous liquid electrolytes for lithium-based rechargeable batteries. *Chem. Rev.* **104**, 4303-4417 (2004).
- 49 Sun, Y.-K. *et al.* High-energy cathode material for long-life and safe lithium batteries. *Nat Mater* **8**, 320-324 (2009).
- 50 Zhang, S. S. A review on electrolyte additives for lithium-ion batteries. *J. Power Sources* **162**, 1379-1394 (2006).
- 51 Ue, M. in *Lithium-Ion Batteries* (eds M. Yoshio, R. J. Brodd, & A. Kozawa) (Springer, New York, 2009).
- 52 Howell, D. *Fiscal year 2010 Annual progress report for energy storage R&D*, [www1.eere.energy.gov](http://www1.eere.energy.gov) (2011).
- 53 Park, M., Zhang, X. C., Chung, M. D., Less, G. B. & Sastry, A. M. A review of conduction phenomena in Li-ion batteries. *J. Power Sources* **195**, 7904-7929 (2010).
- 54 Salomon, M. Solubility problems relating to lithium battery electrolytes. *Pure and Applied Chemistry* **70**, 1905-1912 (1998).
- 55 Tarascon, J. M. & Guyomard, D. New electrolyte compositions stable over the 0 to 5 V voltage range and compatible with the  $\text{Li}_{1+x}\text{Mn}_2\text{O}_4$ /carbon Li-ion cells. *Solid State Ion.* **69**, 293-305 (1994).

- 56 Dudley, J. T. *et al.* Conductivity of electrolytes for rechargeable lithium batteries. *J. Power Sources* **35**, 59-82 (1991).
- 57 Elliott, W. E., Hsu, S.-L. & Towle, W. A program to develop a high-energy density primary battery with a minimum of 200 watt hours per pound of total battery weight. *NASA report 65N11518* (1964).
- 58 Pistoia, G., De Rossi, M. & Scrosati, B. Study of the Behavior of Ethylene Carbonate as a Nonaqueous Battery Solvent. *J. Electrochem. Soc.* **117**, 500-502 (1970).
- 59 Pistoia, G. Nonaqueous Batteries with LiClO<sub>4</sub>-Ethylene Carbonate as Electrolyte. *J. Electrochem. Soc.* **118**, 153-158 (1971).
- 60 Guyomard, D. & Tarascon, J. M. Rechargeable Li<sub>1+x</sub>Mn<sub>2</sub>O<sub>4</sub>/Carbon Cells with a New Electrolyte Composition. *J. Electrochem. Soc.* **140**, 3071-3081 (1993).
- 61 Johnson, B. A. & White, R. E. Characterization of commercially available lithium-ion batteries. *J. Power Sources* **70**, 48-54 (1998).
- 62 Song, J. Y., Wang, Y. Y. & Wan, C. C. Review of gel-type polymer electrolytes for lithium-ion batteries. *J. Power Sources* **77**, 183-197 (1999).
- 63 Tarascon, J. M., Gozdz, A. S., Schmutz, C., Shokoohi, F. & Warren, P. C. Performance of Bellcore's plastic rechargeable Li-ion batteries. *Solid State Ion.* **86-88**, 49-54 (1996).
- 64 Armand, M. The history of polymer electrolytes. *Solid State Ion.* **69**, 309-319 (1994).
- 65 Armand, M. B., Chabagno, J. M. & Duclot, M. J. in *Fast ion transport in solids* (eds P. Vashishta, J.N. Mundy, & G.K. Shenoy) p. 131 (North Holland, Amsterdam, 1979).
- 66 Fenton, D. E., Parker, J. M. & Wright, P. V. Complexes of alkali metal ions with poly(ethylene oxide). *Polymer* **14**, 589-589 (1973).
- 67 Gray, F. M. *Polymer electrolytes*. (The Royal Society of Chemistry, 1997).
- 68 Hooper, A. & North, J. M. The fabrication and performance of all solid state polymer-based rechargeable lithium cells. *Solid State Ion.* **9-10**, 1161-1166 (1983).
- 69 Fergus, J. W. Ceramic and polymeric solid electrolytes for lithium-ion batteries. *J. Power Sources* **195**, 4554-4569 (2010).
- 70 Ahmad, S. Polymer electrolytes: characteristics and peculiarities. *Ionics* **15**, 309-321 (2009).
- 71 Ciosek, M. *et al.* Ion transport phenomena in polymeric electrolytes. *Electrochim. Acta* **53**, 1409-1416 (2007).
- 72 Scrosati, B., Croce, F. & Panero, S. Progress in lithium polymer battery R&D. *J. Power Sources* **100**, 93-100 (2001).
- 73 Syzdek, J. *et al.* Detailed studies on the fillers modification and their influence on composite, poly(oxyethylene)-based polymeric electrolytes. *Electrochim. Acta* **55**, 1314-1322 (2010).
- 74 Damen, L., Hassoun, J., Mastragostino, M. & Scrosati, B. Solid-state, rechargeable Li/LiFePO<sub>4</sub> polymer battery for electric vehicle application. *J. Power Sources* **195**, 6902-6904 (2010).
- 75 Angell, C. A., Liu, C. & Sanchez, E. Rubbery Solid Electrolytes with Dominant Cationic Transport and High Ambient Conductivity. *Nature* **362**, 137-139 (1993).
- 76 Syzdek, J. *et al.* Ceramic-in-polymer versus polymer-in-ceramic polymeric electrolytes-A novel approach. *J. Power Sources* **194**, 66-72 (2009).
- 77 Ohno, H. Functional design of ionic liquids. *Bull. Chem. Soc. Jpn.* **79**, 1665-1680 (2006).
- 78 Armand, M., Endres, F., MacFarlane, D. R., Ohno, H. & Scrosati, B. Ionic-liquid materials for the electrochemical challenges of the future. *Nat. Mater.* **8**, 621-629 (2009).
- 79 Lewandowski, A. & Swiderska-Mocek, A. Ionic liquids as electrolytes for Li-ion batteries-An overview of electrochemical studies. *J. Power Sources* **194**, 601-609 (2009).
- 80 Koch, V. *Covalent Associates* (Santa Clara, CA, USA, 2011).
- 81 Sowmiah, S., Srinivasadesikan, V., Tseng, M. C. & Chu, Y. H. On the Chemical Stabilities of Ionic Liquids. *Molecules* **14**, 3780-3813 (2009).
- 82 Ue, M., Tokuda, H., Kawai, T., Yanagidate, M. & Otake, Y. Thermal Behavior of Ionic Liquid Electrolytes in Lithium-ion Cells. *ECS Transactions* **16**, 173-181 (2009).
- 83 Hori, M., Aoki, Y., Maeda, S., Tatsumi, R. & Hayakawa, S. Thermal Stability of Ionic Liquids as an Electrolyte for Lithium-Ion Batteries. *ECS Transactions* **25**, 147-153 (2010).
- 84 Fuller, J., Breda, A. C. & Carlin, R. T. Ionic liquid-polymer gel electrolytes. *J. Electrochem. Soc.* **144**, L67-L70 (1997).
- 85 Shin, J.-H., Henderson, W. A. & Passerini, S. Ionic liquids to the rescue? Overcoming the ionic conductivity limitations of polymer electrolytes. *Electrochemistry Communications* **5**, 1016-1020 (2003).

- 86 Lane, G. H. *et al.* The electrochemistry of lithium in ionic liquid/organic diluent mixtures. *Electrochim. Acta* **55**, 8947-8952 (2010).
- 87 Bayley, P. M., Best, A. S., MacFarlane, D. R. & Forsyth, M. The effect of coordinating and non-coordinating additives on the transport properties in ionic liquid electrolytes for lithium batteries. *Phys. Chem. Chem. Phys.* **13**, 4632-4640 (2011).
- 88 Bayley, P. M., Lane, G. H., Lyons, L. J., MacFarlane, D. R. & Forsyth, M. Undoing Lithium Ion Association in Ionic Liquids through the Complexation by Oligoethers. *J. Phys. Chem. C* **114**, 20569-20576 (2010).
- 89 Lane, G. H., Best, A. S., MacFarlane, D. R., Forsyth, M. & Hollenkamp, A. F. On the role of cyclic unsaturated additives on the behaviour of lithium metal electrodes in ionic liquid electrolytes. *Electrochim. Acta* **55**, 2210-2215 (2010).
- 90 Egashira, M. *et al.* The preparation of quaternary ammonium-based ionic liquid containing a cyano group and its properties in a lithium battery electrolyte. *J. Power Sources* **138**, 240-244 (2004).
- 91 Matsumoto, H., Sakaebe, H. & Tatsumi, K. Preparation of room temperature ionic liquids based on aliphatic onium cations and asymmetric amide anions and their electrochemical properties as a lithium battery electrolyte. *J. Power Sources* **146**, 45-50 (2005).
- 92 Bhatt, A. I., Best, A. S., Huang, J. & Hollenkamp, A. F. Application of the N-propyl-N-methylpyrrolidinium Bis(fluorosulfonyl)imide RTIL Containing Lithium Bis(fluorosulfonyl)imide in Ionic Liquid Based Lithium Batteries. *J. Electrochem. Soc.* **157**, A66-A74 (2010).
- 93 Vallée, A., Besner, S. & Prud'Homme, J. Comparative study of poly(ethylene oxide) electrolytes made with LiN(CF<sub>3</sub>SO<sub>2</sub>)<sub>2</sub>, LiCF<sub>3</sub>SO<sub>3</sub> and LiClO<sub>4</sub>: Thermal properties and conductivity behaviour. *Electrochim. Acta* **37**, 1579-1583 (1992).
- 94 Dominey, L. A., Koch, V. R. & Blakley, T. J. Thermally stable lithium salts for polymer electrolytes. *Electrochim. Acta* **37**, 1551-1554 (1992).
- 95 Marom, R., Haik, O., Aurbach, D. & Halalay, I. C. Revisiting LiClO<sub>4</sub> as an Electrolyte for Rechargeable Lithium-Ion Batteries. *J. Electrochem. Soc.* **157**, A972-A983 (2010).
- 96 Zhang, S. S., Xu, K. & Jow, T. R. A Thermal Stabilizer for LiPF<sub>6</sub>-Based Electrolytes of Li-Ion Cells. *Electrochemical and Solid-State Letters* **5**, A206-A208 (2002).
- 97 Sloop, S. E., Pugh, J. K., Wang, S., Kerr, J. B. & Kinoshita, K. Chemical Reactivity of PF<sub>5</sub> and LiPF<sub>6</sub> in Ethylene Carbonate/Dimethyl Carbonate Solutions. *Electrochemical and Solid-State Letters* **4**, A42-A44 (2001).
- 98 Hammami, A., Raymond, N. & Armand, M. Runaway risk of forming toxic compounds. *Nature* **424**, 635 (2003).
- 99 Ravidel, B. *et al.* Thermal stability of lithium-ion battery electrolytes. *J. Power Sources* **119-121**, 805-810 (2003).
- 100 Campion, C. L., Li, W. T. & Lucht, B. L. Thermal decomposition of LiPF<sub>6</sub>-based electrolytes for lithium-ion batteries. *J. Electrochem. Soc.* **152**, A2327 (2005).
- 101 Gachot, G. *et al.* Gas Chromatography/Mass Spectrometry As a Suitable Tool for the Li-Ion Battery Electrolyte Degradation Mechanisms Study. *Anal. Chem.* **83**, 478-485 (2011).
- 102 Xu, K., Zhang, S. S., Jow, T. R., Xu, W. & Angell, C. A. LiBOB as salt for lithium-ion batteries - A possible solution for high temperature operation. *Electrochem. Solid State Lett.* **5**, A26-A29 (2002).
- 103 Xu, K., Zhang, S. S. & Jow, R. Electrochemical impedance study of graphite/electrolyte interface formed in LiBOB/PC electrolyte. *J. Power Sources* **143**, 197-202 (2005).
- 104 Xu, K., Zhang, S. S., Lee, U., Allen, J. L. & Jow, T. R. LiBOB: Is it an alternative salt for lithium ion chemistry? *J. Power Sources* **146**, 79-85 (2005).
- 105 Xu, K. Tailoring electrolyte composition for LiBOB. *J. Electrochem. Soc.* **155**, A733-A738 (2008).
- 106 Hassoun, J., Wachtler, M., Wohlfahrt-Mehrens, M. & Scrosati, B. Electrochemical behaviour of Sn and Sn-C composite electrodes in LiBOB containing electrolytes. *J. Power Sources* **196**, 349-354 (2011).
- 107 Liu, J., Chen, Z., Busking, S. & Amine, K. Lithium difluoro(oxalato)borate as a functional additive for lithium-ion batteries. *Electrochemistry Communications* **9**, 475-479 (2007).
- 108 Shui Zhang, S. An unique lithium salt for the improved electrolyte of Li-ion battery. *Electrochemistry Communications* **8**, 1423-1428 (2006).
- 109 Zugmann, S. *et al.* Electrochemical characterization of electrolytes for lithium-ion batteries based on lithium difluoromono(oxalato)borate. *J. Power Sources* **196**, 1417-1424 (2011).

- 110 Li, J. *et al.* Lithium oxalyldifluoroborate/carbonate electrolytes for LiFePO<sub>4</sub>/artificial graphite lithium-ion cells. *J. Power Sources* **195**, 5344-5350 (2010).
- 111 Fu, M. H., Huang, K. L., Liu, S. Q., Liu, J. S. & Li, Y. K. Lithium difluoro(oxalato)borate/ethylene carbonate + propylene carbonate + ethyl(methyl) carbonate electrolyte for LiMn<sub>2</sub>O<sub>4</sub> cathode. *J. Power Sources* **195**, 862-866 (2010).
- 112 Zhang, Z. *et al.* LiPF<sub>6</sub> and lithium oxalyldifluoroborate blend salts electrolyte for LiFePO<sub>4</sub>/artificial graphite lithium-ion cells. *J. Power Sources* **195**, 7397-7402 (2010).
- 113 Zygadlo-Monikowska, E. *et al.* Mixture of LiBF<sub>4</sub> and lithium difluoro(oxalato)borate for application as a new electrolyte for lithium-ion batteries. *J. Power Sources* **195**, 6202-6206 (2010).
- 114 Wietelmann, U. *et al.* Tris (oxalato) phosphorus acid and its lithium salt. *Chemistry-a European Journal* **10**, 2451-2458 (2004).
- 115 Markusson, H., Johansson, P. & Jacobsson, P. Electrochemical stability and lithium ion-anion interactions of orthoborate anions (BOB, MOB, BMB), and presentation of a novel anion: Tris-oxalato-phosphate. *Electrochem. Solid State Lett.* **8**, A215-A218 (2005).
- 116 Xiao, A., Yang, L. & Lucht, B. L. Thermal Reactions of LiPF<sub>6</sub> with Added LiBOB. *Electrochemical and Solid-State Letters* **10**, A241-A244 (2007).
- 117 Xu, M., Xiao, A., Li, W. & Lucht, B. L. Investigation of Lithium Tetrafluorooxalatophosphate [LiPF<sub>4</sub>(C<sub>2</sub>O<sub>4</sub>)] as a Lithium-Ion Battery Electrolyte for Elevated Temperature Performance. *J. Electrochem. Soc.* **157**, A115-A120 (2010).
- 118 Kita, F. *et al.* Electronic structures and electrochemical properties of LiPF<sub>6</sub>-n(CF<sub>3</sub>)<sub>n</sub>. *J. Power Sources* **97-98**, 581-583 (2001).
- 119 Schmidt, M. *et al.* Lithium fluoroalkylphosphates: a new class of conducting salts for electrolytes for high energy lithium-ion batteries. *J. Power Sources* **97-98**, 557-560 (2001).
- 120 Zhou, Z.-B., Takeda, M. & Ue, M. Novel electrolyte salts based on perfluoroalkyltrifluoroborate anions: 1. Synthesis and characterization. *Journal of Fluorine Chemistry* **123**, 127-131 (2003).
- 121 Gnanaraj, J. S., Levi, M. D., Gofer, Y., Aurbach, D. & Schmidt, M. LiPF<sub>3</sub>(CF<sub>2</sub>CF<sub>3</sub>)(<sub>3</sub>): A salt for rechargeable lithium ion batteries. *J. Electrochem. Soc.* **150**, A445-A454 (2003).
- 122 Zhou, Z.-B., Takeda, M., Fujii, T. & Ue, M. Li[C<sub>2</sub>F<sub>5</sub>]BF<sub>3</sub>] as an Electrolyte Salt for 4 V Class Lithium-Ion Cells. *J. Electrochem. Soc.* **152**, A351-A356 (2005).
- 123 Ue, M., Fujii, T., Zhou, Z. B., Takeda, M. & Kinoshita, S. Electrochemical properties of Li[C<sub>n</sub>F<sub>2n+1</sub>BF<sub>3</sub>] as electrolyte salts for lithium-ion cells. *Solid State Ion.* **177**, 323-331 (2006).
- 124 Yang, H., Kwon, K., Devine, T. M. & Evans, J. W. Aluminum Corrosion in Lithium Batteries An Investigation Using the Electrochemical Quartz Crystal Microbalance. *J. Electrochem. Soc.* **147**, 4399-4407 (2000).
- 125 Krause, L. J. *et al.* Corrosion of aluminum at high voltages in non-aqueous electrolytes containing perfluoroalkylsulfonyl imides; new lithium salts for lithium-ion cells. *J. Power Sources* **68**, 320-325 (1997).
- 126 Kanamura, K. Anodic oxidation of nonaqueous electrolytes on cathode materials and current collectors for rechargeable lithium batteries. *J. Power Sources* **81-82**, 123-129 (1999).
- 127 Kanamura, K., Umegaki, T., Shiraishi, S., Ohashi, M. & Takehara, Z. I. Electrochemical behavior of Al current collector of rechargeable lithium batteries in propylene carbonate with LiCF<sub>3</sub>SO<sub>3</sub>, Li(CF<sub>3</sub>SO<sub>2</sub>)<sub>2</sub>N, or Li(c<sub>4</sub>F<sub>9</sub>SO<sub>2</sub>)(CF<sub>3</sub>SO<sub>2</sub>)N. *J. Electrochem. Soc.* **149**, A185-A194 (2002).
- 128 Han, H. *et al.* Lithium (fluorosulfonyl)(nonafluorobutanesulfonyl)imide (LiFNFSI) as conducting salt to improve the high-temperature resilience of lithium-ion cells. *Electrochemistry Communications* **13**, 265-268 (2011).
- 129 Ruff, J. K. The Imidodisulfonyl Fluoride Ion. *Inorg. Chem.* **4**, 1446-1449 (1965).
- 130 Michot, C., Armand, M., Sanchez, J.-Y., Choquette, Y. & Gauthier, M. Ionic conducting material having good anticorrosive properties, Patent WO9526056. (1995).
- 131 Abouimrane, A., Ding, J. & Davidson, I. J. Liquid electrolyte based on lithium bis-fluorosulfonyl imide salt: Aluminum corrosion studies and lithium ion battery investigations. *J. Power Sources* **189**, 693-696 (2009).
- 132 Han, H.-B. *et al.* Lithium bis(fluorosulfonyl)imide (LiFSI) as conducting salt for nonaqueous liquid electrolytes for lithium-ion batteries: Physicochemical and electrochemical properties. *J. Power Sources* **196**, 3623-3632 (2011).
- 133 Paillard, E. *et al.* Electrochemical and Physicochemical Properties of PY14FSI-Based Electrolytes with LiFSI. *J. Electrochem. Soc.* **156**, A891-A895 (2009).

- 134 Ishikawa, M., Sugimoto, T., Kikuta, M., Ishiko, E. & Kono, M. Pure ionic liquid electrolytes compatible with a graphitized carbon negative electrode in rechargeable lithium-ion batteries. *J. Power Sources* **162**, 658-662 (2006).
- 135 Sugimoto, T. *et al.* Ionic liquid electrolyte systems based on bis(fluorosulfonyl)imide for lithium-ion batteries. *J. Power Sources* **189**, 802-805 (2009).
- 136 Huang, J. & Hollenkamp, A. F. Thermal Behavior of Ionic Liquids Containing the FSI Anion and the Li<sup>+</sup> Cation. *The Journal of Physical Chemistry C* **114**, 21840-21847 (2010).
- 137 Zaghbi, K. *et al.* LiFePO<sub>4</sub> safe Li-ion polymer batteries for clean environment. *J. Power Sources* **146**, 380-385 (2005).
- 138 Egashira, M., Scrosati, B., Armand, M., Beranger, S. & Michot, C. Lithium dicyanotriazolate as a lithium salt for poly(ethylene oxide) based polymer electrolytes. *Electrochem. Solid State Lett.* **6**, A71-A73 (2003).
- 139 Johansson, P., Nilsson, H., Jacobsson, P. & Armand, M. Novel Huckel stabilised azole ring-based lithium salts studied by ab initio Gaussian-3 theory. *Phys. Chem. Chem. Phys.* **6**, 895-899 (2004).
- 140 Niedzicki, L. *et al.* New type of imidazole based salts designed specifically for lithium ion batteries. *Electrochim. Acta* **55**, 1450-1454 (2010).
- 141 Niedzicki, L. *et al.* Modern generation of polymer electrolytes based on lithium conductive imidazole salts. *J. Power Sources* **192**, 612-617 (2009).
- 142 Niedzicki, L., Kasprzyk, M., Kuziak, K., Żukowska, G.Z., Marcinek, M., Wieczorek, W., Armand, M. Liquid electrolytes based on new lithium conductive imidazole salt. *J. Power Sources* **196**, 1386 (2011).
- 143 Johansson, P. Intrinsic anion oxidation potentials. *J. Phys. Chem. A* **111**, 1378-1379 (2007).
- 144 Johansson, P. Intrinsic anion oxidation potentials. *J. Phys. Chem. A* **110**, 12077-12080 (2006).
- 145 Kohanoff, J. *Electronic structure calculations for solids and molecules.* (Cambridge University Press, 2006).
- 146 Jensen, F. *Introduction to Computational Chemistry.* Second Edition edn, (John Wiley & Sons Ltd, 2007).
- 147 Echenique, P. & Alonso, J. L. A mathematical and computational review of Hartree-Fock SCF methods in quantum chemistry. *Molecular Physics: An International Journal at the Interface Between Chemistry and Physics* **105**, 3057 - 3098 (2007).
- 148 Moller, C. & Plesset, M. S. Note on an Approximation Treatment for Many-Electron Systems. *Physical Review* **46**, 618 (1934).
- 149 Cramer, C. *Essentials of Computational Chemistry 2nd ed.* Second Edition edn, (John Wiley & Sons Ltd, 2004).
- 150 Hohenberg, P. & Kohn, W. Inhomogeneous Electron Gas. *Phys. Rev. B* **136**, B864 (1964).
- 151 Kohn, W. & Sham, L. J. Self-Consistent Equations Including Exchange and Correlation Effects. *Physical Review* **140**, 1133-& (1965).
- 152 Perdew, J. P., Ruzsinszky, A., Constantin, L. A., Sun, J. W. & Csonka, G. I. Some Fundamental Issues in Ground-State Density Functional Theory: A Guide for the Perplexed. *Journal of Chemical Theory and Computation* **5**, 902-908 (2009).
- 153 Perdew, J. P., Tao, J., Staroverov, V. N. & Scuseria, G. E. Meta-generalized gradient approximation: Explanation of a realistic nonempirical density functional. *The Journal of Chemical Physics* **120**, 6898-6911 (2004).
- 154 Van Voorhis, T. & Scuseria, G. E. A novel form for the exchange-correlation energy functional. *J. Chem. Phys.* **109**, 400-410 (1998).
- 155 Stephens, P. J., Devlin, F. J., Chabalowski, C. F. & Frisch, M. J. Ab-Initio Calculation of Vibrational Absorption and Circular-Dichroism Spectra Using Density-Functional Force-Fields. *J. Phys. Chem.* **98**, 11623-11627 (1994).
- 156 Sousa, S. F., Fernandes, P. A. & Ramos, M. J. General performance of density functionals. *J. Phys. Chem. A* **111**, 10439-10452 (2007).
- 157 Perdew, J. P. & Ruzsinszky, A. Fourteen easy lessons in density functional theory. *International Journal of Quantum Chemistry* **110**, 2801-2807 (2010).
- 158 Tomasi, J., Mennucci, B. & Cammi, R. Quantum Mechanical Continuum Solvation Models. *Chem. Rev.* **105**, 2999-3094 (2005).
- 159 Miertus, S., Scrocco, E. & Tomasi, J. Electrostatic interaction of a solute with a continuum. A direct utilization of ab initio molecular potentials for the prevision of solvent effects. *Chemical Physics* **55**, 117-129 (1981).

- 160 Klamt, A. & Schuurmann, G. COSMO: a new approach to dielectric screening in solvents with explicit expressions for the screening energy and its gradient. *Journal of the Chemical Society, Perkin Transactions 2*, 799-805 (1993).
- 161 Barone, V. & Cossi, M. Quantum calculation of molecular energies and energy gradients in solution by a conductor solvent model. *J. Phys. Chem. A* **102**, 1995-2001 (1998).
- 162 Bondi, A. van der Waals Volumes and Radii. *The Journal of Physical Chemistry* **68**, 441-451 (1964).
- 163 Batsanov, S. S. Van der Waals Radii of Elements. *Inorganic Materials* **37**, 871-885-885 (2001).
- 164 Tomasi, J. in *Continuum Solvation Models in Chemical Physics* (eds B. Mennucci & R. Cammi) (John Wiley & Sons, Chichester, England., 2007).
- 165 Canongia Lopes, J. N. *et al.* Potential Energy Landscape of Bis(fluorosulfonyl)amide. *The Journal of Physical Chemistry B* **112**, 9449-9455 (2008).
- 166 Yamaguchi, Y., Frisch, M., Gaw, J., Schaefer Iii, H. F. & Binkley, J. S. Analytic evaluation and basis set dependence of intensities of infrared spectra. *The Journal of Chemical Physics* **84**, 2262-2278 (1986).
- 167 Frisch, M. J., Yamaguchi, Y., Gaw, J. F., Schaefer Iii, H. F. & Binkley, J. S. Analytic Raman intensities from molecular electronic wave functions. *The Journal of Chemical Physics* **84**, 531-532 (1986).
- 168 Johansson, P. & Jacobsson, P. Rational design of electrolyte components by ab initio calculations. *J. Power Sources* **153**, 336-344 (2006).
- 169 Kita, F., Kawakami, A., Sonoda, T. & Kobayashi, H. in *New Sealed Rechargeable Batteries and Supercapacitors, PV 93-23, p. 321* (eds B.M. Barnett *et al.*) (The Electrochemical Society Proceeding Series, Pennington, NJ, 1993).
- 170 Ue, M., Murakami, A. & Nakamura, S. Anodic stability of several anions examined by ab initio molecular orbital and density functional theories. *J. Electrochem. Soc.* **149**, A1572-A1577 (2002).
- 171 Hollas, J. M. *Modern Spectroscopy, third edition.* (John Wiley & Sons, 1996).
- 172 Kim, C. K. *et al.* Density functional theory studies on the dissociation energies of metallic salts: relationship between lattice and dissociation energies. *Journal of Computational Chemistry* **22**, 827-834 (2001).
- 173 Zakhevskii, V. G., Boldyrev, A. I. & Charkin, O. P. AB initio calculations of the structure and stability of the non-rigid LiBF<sub>4</sub> molecule. *Chemical Physics Letters* **73**, 54-57 (1980).
- 174 Francisco, J. S. & Williams, I. H. Structural and Spectral Consequences of Ion-Pairing .4. Theoretical-Study of Bf<sub>4</sub>-Li+, Bf<sub>4</sub>-Na+, Bf<sub>4</sub>-K+, Bf<sub>4</sub>-Rb+. *J. Phys. Chem.* **94**, 8522-8529 (1990).
- 175 Mennucci, B., Cancès, E. & Tomasi, J. Evaluation of Solvent Effects in Isotropic and Anisotropic Dielectrics and in Ionic Solutions with a Unified Integral Equation Method: Theoretical Bases, Computational Implementation, and Numerical Applications. *The Journal of Physical Chemistry B* **101**, 10506-10517 (1997).
- 176 Johansson, P. & Jacobsson, P. Ion Pairs in Polymer Electrolytes Revisited: An Ab Initio Study. *The Journal of Physical Chemistry A* **105**, 8504-8509 (2001).
- 177 Xuan, X. P., Zhang, H. C., Wang, J. J. & Wang, H. Q. Vibrational spectroscopic and density functional studies on ion solvation and association of lithium tetrafluoroborate in acetonitrile. *J. Phys. Chem. A* **108**, 7513-7521 (2004).
- 178 Xuan, X. P., Wang, J. J., Zhao, Y. & Zhu, J. J. Experimental and computational studies on the solvation of lithium tetrafluoroborate in dimethyl sulfoxide. *J. Raman Spectrosc.* **38**, 865-872 (2007).
- 179 Johansson, P. & Jacobsson, P. Lithium salt dissociation in non-aqueous electrolytes modeled by ab initio calculations. *Solid State Ion.* **177**, 2691-2697 (2006).
- 180 Johansson, P. Electronic structure calculations on lithium battery electrolyte salts. *Phys. Chem. Chem. Phys.* **9**, 1493-1498 (2007).
- 181 Ue, M., Murakami, A. & Nakamura, S. A convenient method to estimate ion size for electrolyte materials design (vol 149, pg A1385, 2002). *J. Electrochem. Soc.* **150**, L1-L1 (2003).
- 182 Long, D. A. *The Raman Effect.* (John Wiley & Sons, 2002).
- 183 Raman, C. V. & Krishnan, K. S. A New Type of Secondary Radiation. *Nature* **121**, 501-502 (1928).
- 184 Brodd, R. J. in *Lithium-Ion Batteries* (eds M. Yoshio, R. J. Brodd, & A. Kozawa) (Springer, New York, 2009).
- 185 Horiba, T. in *Lithium-Ion Batteries* (eds M. Yoshio, R. J. Brodd, & A. Kozawa) (Springer, New York, 2009).
- 186 Chevrolet Volt, [www.chevrolet.com/volt](http://www.chevrolet.com/volt)

- 187 Conley, P. J. & Hickman, J. The green car report. (MDB Capital Group, Santa Monica, CA, USA, 2008).
- 188 ThInk. [www.thinkev.com](http://www.thinkev.com)
- 189 Ener1. *Ener1 Achieves Milestone with Volvo's C30 Electric Vehicle*, [www.ener1.com](http://www.ener1.com) 2011 (11 Jan)
- 190 A123. *A123 Systems Selected to Develop Battery Pack for New Electric Vehicle from Shanghai Automotive Industry Corporation*, [www.a123systems.com](http://www.a123systems.com) (2010 (9 Nov) ).
- 191 Ener1. *Lithium-Ion Battery Maker Ener1 Inc., Partners With Russia's Federal Grid Company to Develop Energy Storage Opportunities on Country's National Power Network*, [www.ener1.com](http://www.ener1.com) (2010 (17 June) ).
- 192 A123. *A123 Systems to Supply 20MW of Advanced Energy Storage Solutions to AES Gener for Spinning Reserve Project in Chile*, [www.a123systems.com](http://www.a123systems.com) (2011 (7 Feb) ).

## A1 ACKNOWLEDGEMENT

Thank you all co-authors for your contribution to this work. A special thanks to Patrik and Per for lots of (and rapid) support, in particular when finalizing this thesis. I've felt comfortable in the open and cheerful working atmosphere you create, sometimes maybe a little too comfortable...

Travelling, I've had the opportunity to get to know some colleagues better, especially fellow PhD-students; Anna M (Brazil, Italy), Jagath (Australia, South Korea), Erlendur (Canada), and Susanne (South Korea). We have shared some really memorable experiences together. Also, travel grants from Adlerbertska forskningsstiftelsen, Ångpanneföreningen, and Stiftelsen Futura, which have made these trips possible, are acknowledged.

The multi-cultural experience has never been far, sharing room with a true Göteborgare; you are a good (and tidy) room-mate Jonas. Also, down the corridor many of you have had to put up with me extracting part of your culture. I mention no names, since I would regret to miss someone out (neither does my keyboard support the necessary characters). Thus, I thank all KMF members – past and present.

Presents, I have brought home in plenty, although I know it is a poor compensation for being away from home. So, last, but not least, kisses and hugs for Nathalie, Kevin, Olivia, and Leah. I love you very much.

27<sup>th</sup> of April 2011

Johan



## A2 APPENDIX

### Li-ion batteries – application status

The Li-ion battery has since its introduction been a great success and rapidly come to dominate the markets of portable electronic devices. In 1991 the worldwide sales of Li-ion batteries was 1 million USD, compared to 39 and 1535 million USD, for NiMH and NiCd batteries, respectively.<sup>184</sup> Already in 1998, the Li-ion battery sales exceeded that of both NiMH and NiCd batteries, and 2005 the value of the Li-ion market was approximately three times that of the NiMH and NiCd markets, combined.<sup>184</sup> This expansion was possible by a simultaneous development of Li-ion battery performance and cost reduction through cell engineering; from 1995 to 2006 the cost of a cylindrical 18 650 cell (diameter 18 mm, length 65.0 mm)<sup>61</sup> was reduced by half, while the energy density was more than doubled.<sup>184</sup> Today billions<sup>33</sup> of Li-ion batteries are produced annually in a range of formats.<sup>12,184</sup> The two most important markets, in terms of the number of cells sold, are cellular phones and notebook computers.<sup>33,184</sup>

It is believed that the performance limit of graphite/LiPF<sub>6</sub> (non-aq)/LiCoO<sub>2</sub> Li-ion batteries was reached during the past decade, but the introduction of alternative electrode materials, especially cathodes, has led to new application areas. With LiMn<sub>2</sub>O<sub>4</sub> or LiFePO<sub>4</sub> cathodes, improved discharge rates have made Li-ion cells contenders for NiCd batteries in the power tool market,<sup>184</sup> offering low self-discharge and improved efficiencies.<sup>10</sup> A combination of new cathode and anode materials have also been a ticket for entrance of Li-ion batteries into the vehicle transportation market, because of higher cell performance, but mainly improved battery safety. The main competition in this market are NiMH type batteries, which were introduced in the early HEVs, but are now being replaced by Li-ion cells by several car manufacturers in future HEV series, for example the Toyota Prius and Segway Transporter.<sup>185</sup> In the Chevrolet Volt E-REV (extended-range electric vehicle) released late 2010, a manganese based cathode and a carbon anode are the active materials of the +200 cell, 16 kWh, 181.4 kg battery.<sup>186</sup> Fully charged, the battery can power the Volt for an average distance ~55 km and has a recharging time from 4 hours.

The battery for the Chevrolet Volt is provided by LG Chem – one of many battery manufacturers that have partnered up with one or several automotive manufacturers to profit on a potential 100 billion USD market.<sup>187</sup> Two examples are Ener1 (EnerDel), developing batteries with a lithium titanium oxide, Li<sub>4</sub>Ti<sub>5</sub>O<sub>12</sub> anode in place of the carbon anode, and A123Systems, who provide batteries with a LiFePO<sub>4</sub> cathode. Ener1 supply batteries to the Norwegian EV company Th!nk, to complement the sodium based ZEBRA battery in the Th!nk City,<sup>188</sup> and since 2009 also to Volvo Cars, for use in

the Volvo C30 EV, which was recently subjected to the first demonstration of a crash-test of a fully charged EV.<sup>189</sup> A123Systems have revealed that they will provide batteries to the largest Chinese automaker,<sup>190</sup> Shanghai Automotive Industry Corporation (SAIC), and supply batteries to Daimler and BMW for electrical buses and trucks.

For the very cost-sensitive market of grid applications or uninterruptible power sources, the lead-acid battery is the dominating battery solution. The main alternative has been more expensive, long-life (>15 yrs) NiCd batteries, as Li-ion cells have been too far from the estimated 0.3 USD/Wh needed.<sup>184</sup> However, both Ener1 and A123Systems provide grid solutions and have initiated collaborations around the world. Ener1 will develop high-performance battery systems for Russia's federal grid company,<sup>191</sup> controlling the world's fourth largest electricity market, and A123Systems is currently providing battery solutions to the Chilean power grid and have announced further stationary projects in Chile.<sup>192</sup>

Thus, over two decades, improved engineering and new electrode materials have developed the Li-ion batteries to the most important power source for consumer electronics and in addition introduced these batteries in many other application areas. However, little progress has been made in the development of the Li-ion battery electrolytes, which are currently based on flammable organic liquids or gels. The state-of-the-art electrolyte is a fuel for thermal runaway reactions and a source of hazardous fluorinated decomposition products – the safety concerns of which increase with the battery size. Therefore, the development of safe electrolyte alternatives is considered a corner stone if lithium batteries are to be successful in the large scale battery application areas (transportation and grid storage).